THE ANTENNA LABORATORY

RESEARCH ACTIVITIES in - - -

Automatic Controls
Microwave Circuits
Terrain Investigations
Wave Propagation
Antennas
Astronautics
Radomes
Echo Area Studies
E M Field Theory
Systems Analysis
Submillimeter Applications

FACILITY FORM 602

N66 10957 (ACCESSION NUMBER)
(THRU)
51 (PAGES)
1 (CODE)
CR 67833 (NASA CR OR TMX OR AD NUMBER)
07 (CATEGORY)

Theoretical Curves of Backscattering Cross Sections of Rough Surfaces for Several Polarization States Using Two Statistical Models

Donald E. Barrick

Grant Number NsG-213-61

1388-20

31 August 1965

Prepared for:
National Aeronautics and Space Administration
Office of Grants and Research Contracts
Washington, D. C. 20546

Department of ELECTRICAL ENGINEERING

GPO PRICE $ ________

CFSTI PRICE(S) $ ________

Hard copy (HC) $3.00

Microfiche (MF) 50

ff 653 July 65

THE OHIO STATE UNIVERSITY
RESEARCH FOUNDATION
Columbus, Ohio

NOTICES

When Government drawings, specifications, or other data are used for any purpose other than in connection with a definitely related Government procurement operation, the United States Government thereby incurs no responsibility nor any obligation whatsoever, and the fact that the Government may have formulated, furnished, or in any way supplied the said drawings, specifications, or other data, is not to be regarded by implication or otherwise as in any manner licensing the holder or any other person or corporation, or conveying any rights or permission to manufacture, use, or sell any patented invention that may in any way be related thereto.

The Government has the right to reproduce, use, and distribute this report for governmental purposes in accordance with the contract under which the report was produced. To protect the proprietary interests of the contractor and to avoid jeopardy of its obligations to the Government, the report may not be released for non-governmental use such as might constitute general publication without the express prior consent of The Ohio State University Research Foundation.

Qualified requesters may obtain copies of this report from the Defense Documentation Center, Cameron Station, Alexandria, Virginia. Department of Defense contractors must be established for DDC services, or have their "need-to-know" certified by the cognizant military agency of their project or contract.

REPORT 1388-20

REPORT
by
THE OHIO STATE UNIVERSITY RESEARCH FOUNDATION
COLUMBUS, OHIO 43212

Sponsor	National Aeronautics & Space Administration Office of Grants and Research Contracts Washington, D. C. 20546
Grant Number	NsG-213-61
Investigation of	Theoretical and Experimental Analysis of the Electromagnetic Scattering and Radiative Properties of Terrain, with Emphasis on Lunar-Like Surfaces
Subject of Report	Theoretical Curves of Backscattering Cross Sections of Rough Surfaces for Several Polarization States Using Two Statistical Models
Submitted by	Donald E. Barrick Antenna Laboratory Department of Electrical Engineering
Date	31 August 1965

The material contained in this report is also used as a dissertation submitted to the Department of Electrical Engineering, The Ohio State University as partial fulfillment for the degree Doctor of Philosophy.

ABSTRACT

10957

Predicted curves of backscattering cross section per unit area (in decibels) of very rough planar surfaces are shown in this report; these curves are plotted directly from equations in Chapter III of Antenna Laboratory Report 1388-18, and their derivation is given there.

Two statistical models for the surface joint probability density function are considered and the curves from each are shown. Results are shown for both perfectly conducting and lossy dielectric surfaces at several values of dielectric constant. The only roughness parameter which affects the shape of the cross section curves for the models considered here is the rms surface slope.

In Report 1388-18, it is shown that depolarization of the incident wave in the backscattering direction does exist in the case of scattering from non-perfectly conducting surfaces, and the relationship for this depolarized component is found. Hence the backscattering cross sections become polarization sensitive. The various cross sections (including the cross or depolarized cross sections) are shown here for both linear and circular polarization states.

The purpose of the report is to provide a set of curves with which one may compare measured curves in an attempt to estimate the parameters and properties of the surface from which the backscattered power was measured.

THEORETICAL CURVES OF BACKSCATTERING CROSS SECTIONS OF ROUGH SURFACES FOR SEVERAL POLARIZATION STATES USING TWO STATISTICAL MODELS

Introduction and Discussion of Statistical Models

It is shown in Report 1388-18 that one can obtain an expression for average backscattering cross section of a rough surface in terms of the joint characteristic function of the random surface height. Thus in order to obtain a functional solution for the backscattering cross section, one must assume a certain form, or statistical model for this joint characteristic function. In order to obtain a choice for the sake of comparison, two statistical models were chosen, and the curves resulting from both are shown in this report.

The joint characteristic function is the two dimensional Fourier transform of the surface height joint probability density function. The joint probability density functions for the surface height chosen for the two models used here are the Gaussian, given by

$$(1) \qquad W_G(\zeta, \zeta') = \frac{1}{2\pi\sigma^2(1-R^2)^{1/2}} \, e^{-(\zeta^2 - 2R\zeta\zeta' + \zeta'^2)/2\sigma^2(1-R^2)} ,$$

and a model involving modified Bessel functions given by

$$(2) \qquad W_B(\zeta, \zeta') = \frac{3}{\pi^2\sigma^2(1-R^2)^{1/2}} \left[\frac{\sqrt{3}\,|\zeta|}{\sigma}\right] \left[\frac{\sqrt{3}\,|\zeta' - R\zeta|}{\sigma(1-R^2)^{1/2}}\right] K_1\left[\frac{\sqrt{3}\,|\zeta|}{\sigma}\right] K_1\left[\frac{\sqrt{3}\,|\zeta' - R\zeta|}{\sigma(1-R^2)^{1/2}}\right] ,$$

where ζ and ζ' are the random surface heights in the z-direction at the points (x, y) and (x', y') respectively, R is the surface height correlation coefficient, and σ^2 is the variance of the surface height.

These two statistical models, though not producing widely differing backscattering cross sections, do offer a choice of models, each of which may fit the measured data from a certain class of surfaces better than the other. For example, the first model employing a Gaussian height joint probability density function has been shown to offer results which compare quite favorably with scattering from the sea surface; the sea surface height itself has a joint probability density function very close to Gaussian for certain sea states, as revealed by direct measurement. The second model offers better agreement with backscattered power from the moon. The models yield solutions for backscattered power which differ chiefly in their behavior near normal incidence, as is evident from the curves.

Both models are used in conjunction with a Gaussian class surface height correlation coefficient, R; such a correlation coefficient is a function of the separation, ρ, between the two points (x, y) and (x', y') on the surface. The Gaussian class refers to all correlation coefficients which are parabolic near the origin such that $R = 1 - \frac{\rho^2}{a^2}$ for small ρ; "a" here denotes the correlation length. The derivation of the solutions employing these models is done in detail in Report 1388-18.

SECTION E*

In this section the predicted curves for backscattering cross section per unit area of a rough planar surface are shown when only circularly polarized waves are transmitted and received. If no roughness is present a right circularly polarized wave will be reflected as a left circularly polarized wave; however, if roughness is present and depolarization takes place, there will be a right circular component in the scattered field also. The converse is true when the incident wave is left circular.

It has been shown in Report 1388-18 that no depolarization of the incident wave takes place if the surface is a perfect conductor when the physical optics analysis is employed. Hence, the backscattering cross section for the depolarized circular component is shown only for the lossy dielectric surfaces.

These curves are plotted from equations (3.10a) and (3.10c) for the perfectly conducting surfaces, and (3.17a) and (3.17b) for the lossy dielectric surfaces.

---

* These sections are lettered E, F, and G here because they have been used as Appendices E, F, and G of a dissertation by this author.

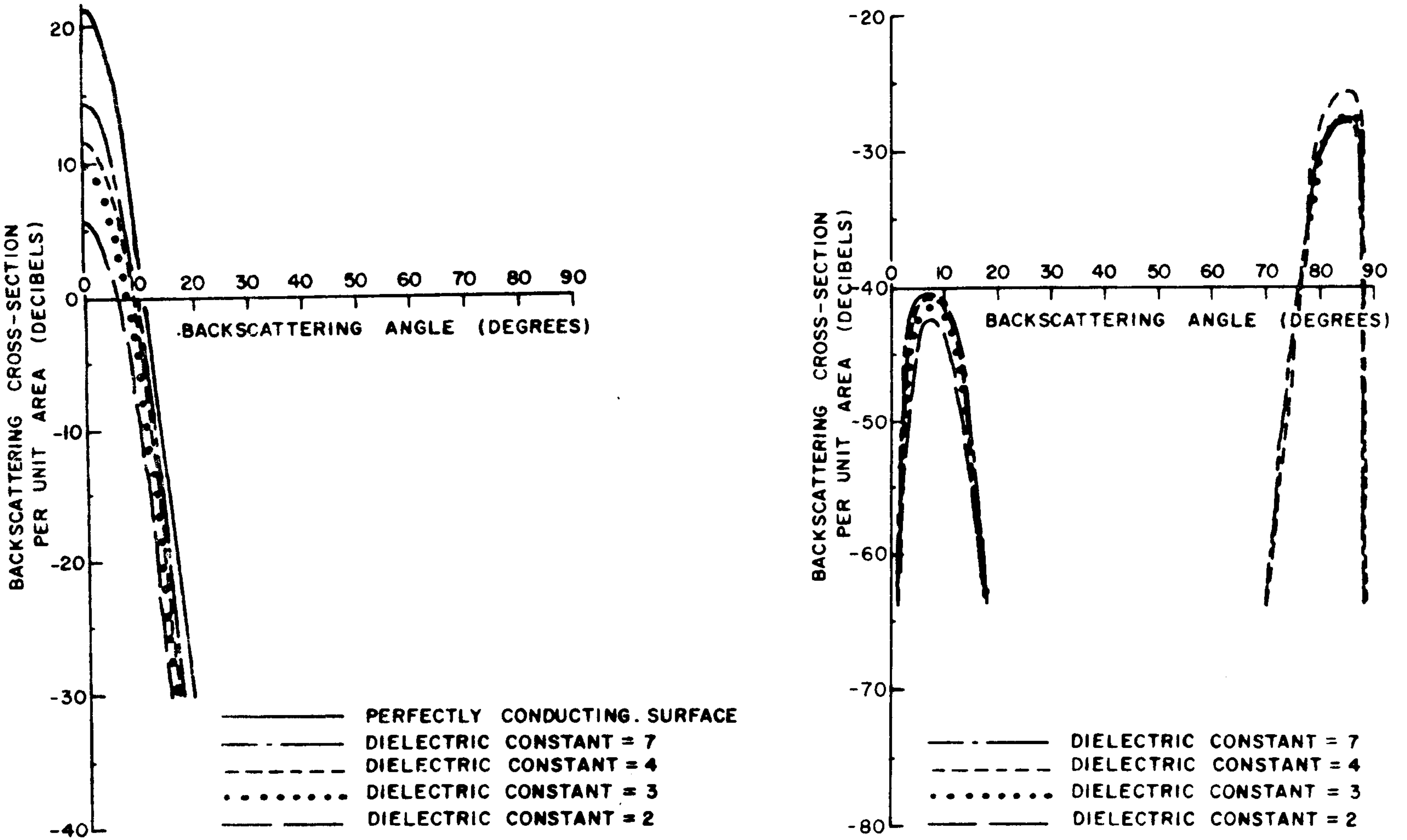

(a) Polarized backscattered component.

(b) Depolarized backscattered component

Fig. E-1--Predicted backscattering cross sections for a rough planar surface using circular polarization. RMS surface slope = 5°. Gaussian JPDF for surface height.

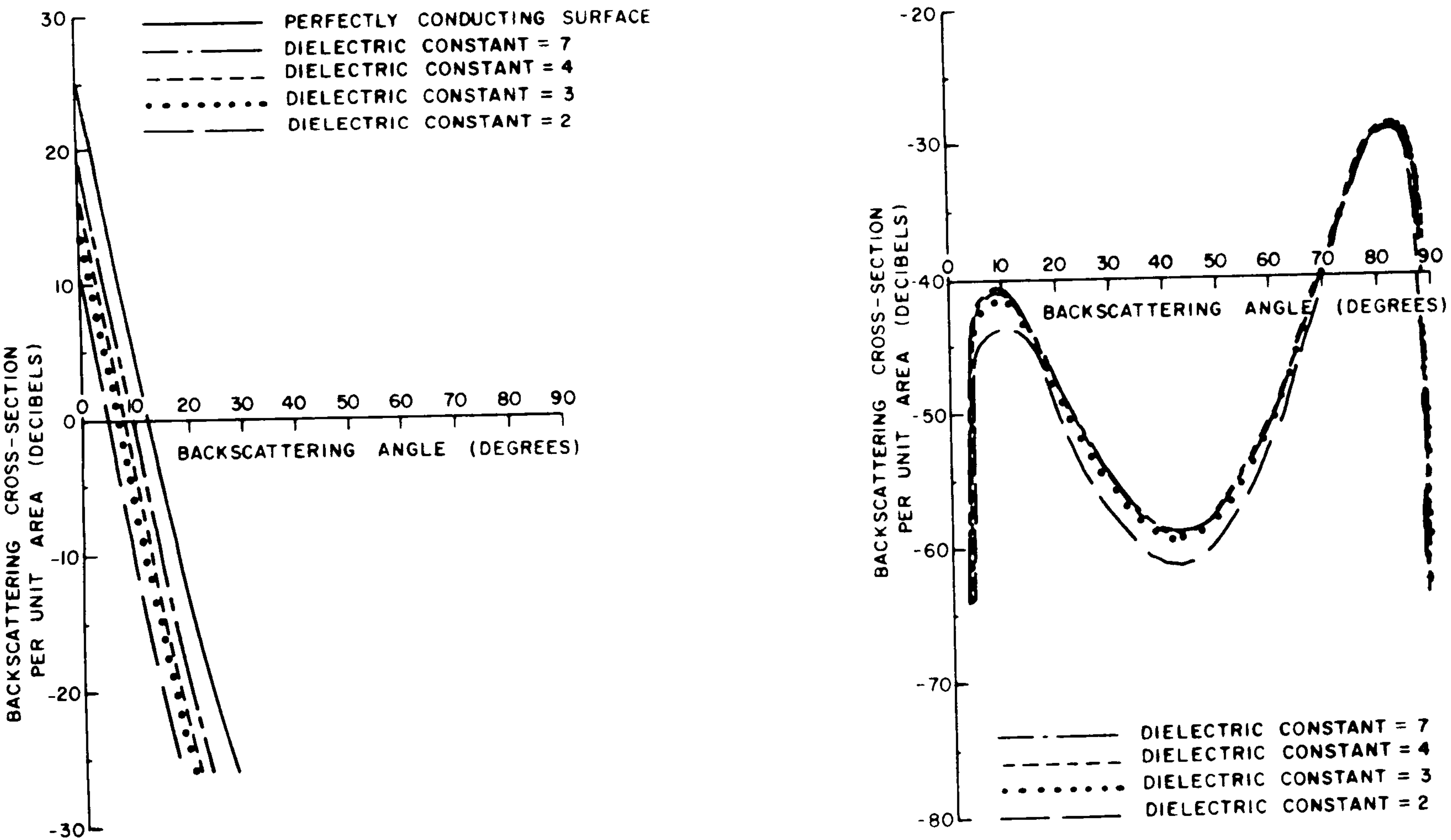

(a) Polarized backscattered component.

(b) Depolarized backscattered component.

Fig. E-2--Predicted backscattering cross sections for a rough planar surface using circular polarization. RMS surface slope = 5°. Bessel JPDF for surface height.

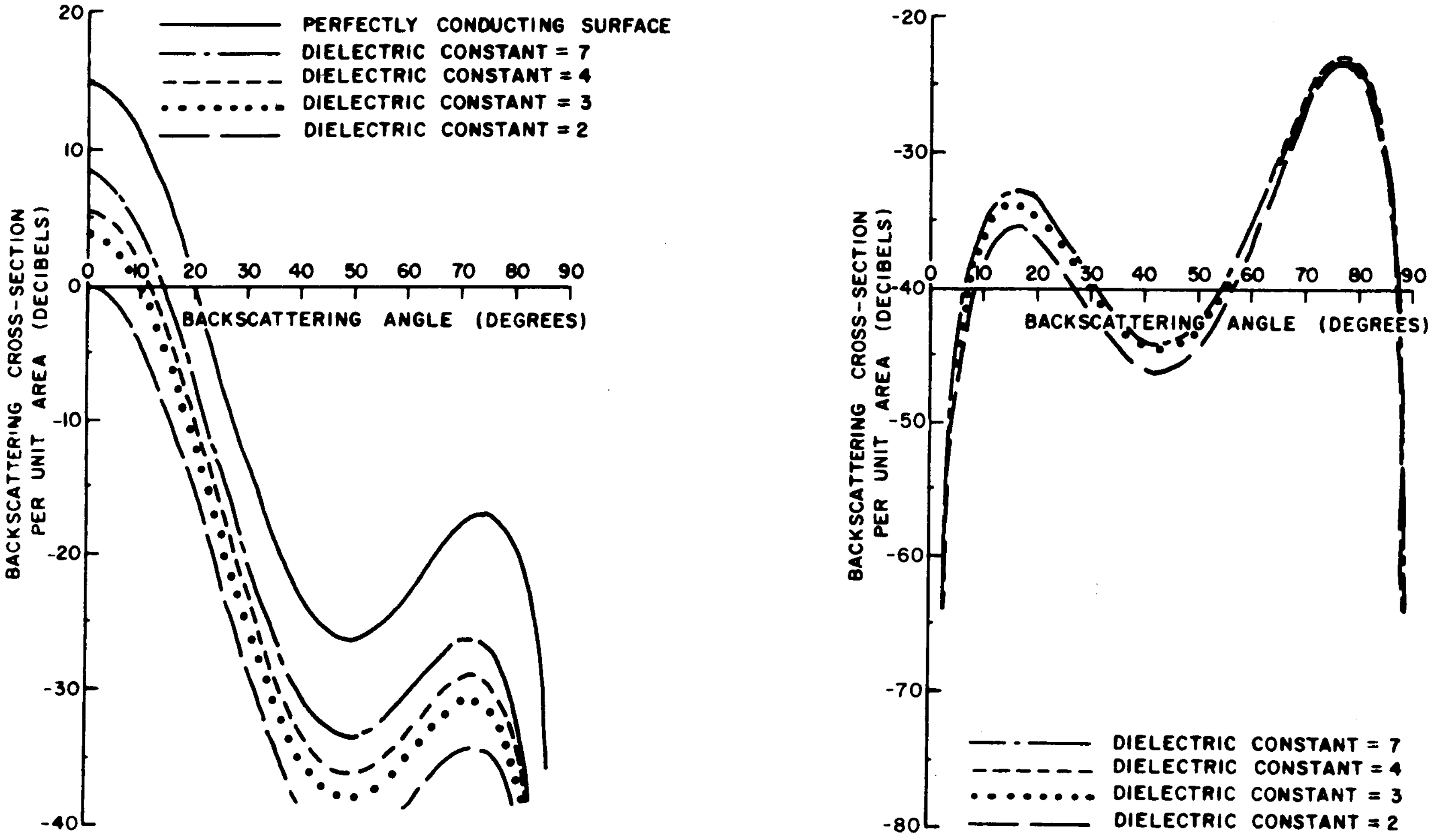

(a) Polarized backscattered component.

(b) Depolarized backscattered component.

Fig. E-3--Predicted backscattering cross sections for a rough planar surface using circular polarization. RMS surface slope = 10°. Gaussian JPDF for surface height.

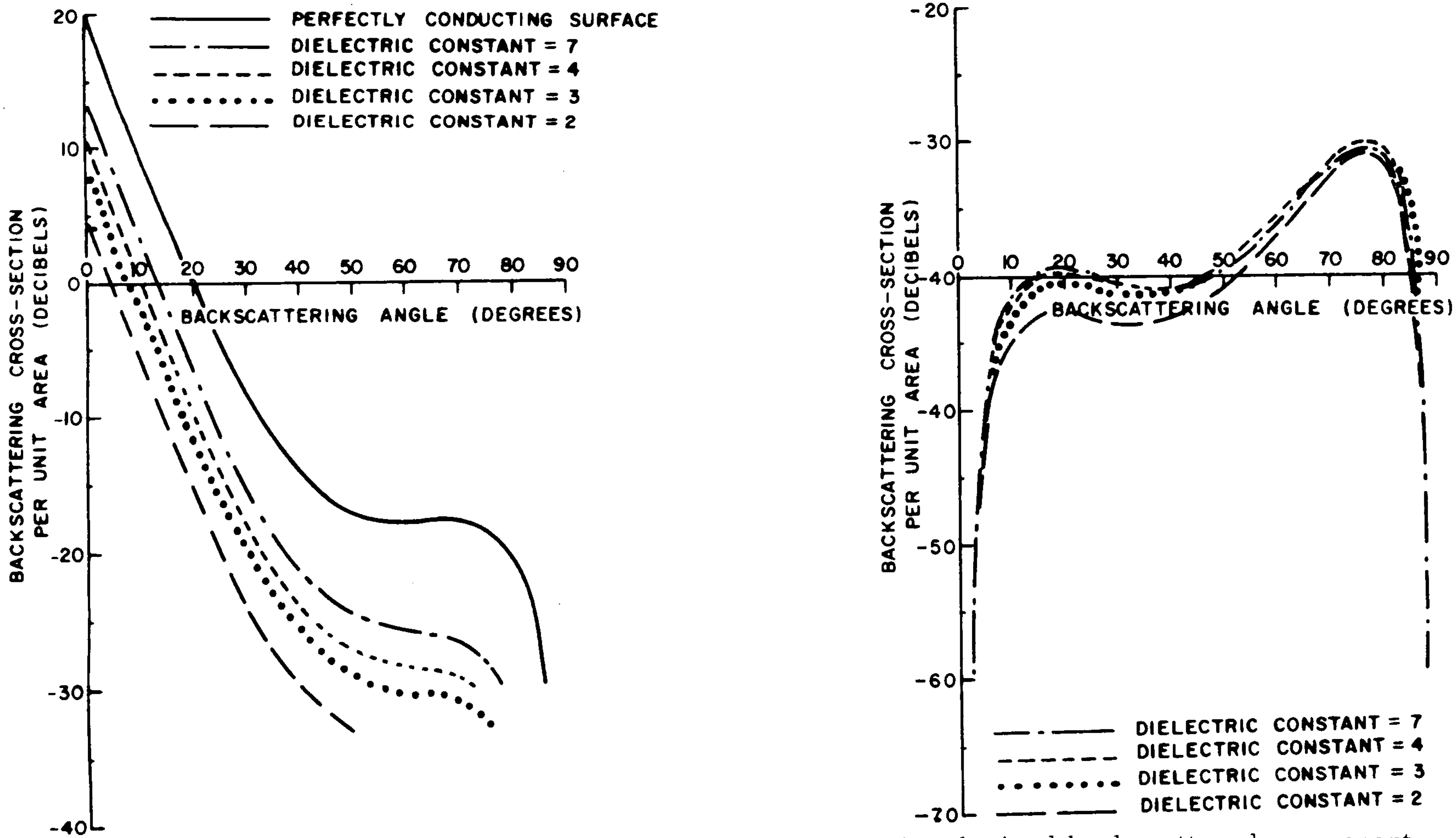

(a) Polarized backscattered component.

(b) Depolarized backscattered component.

Fig. E-4--Predicted backscattering cross sections for a rough planar surface using circular polarization. RMS surface slope = 10°. Bessel JPDF for surface height.

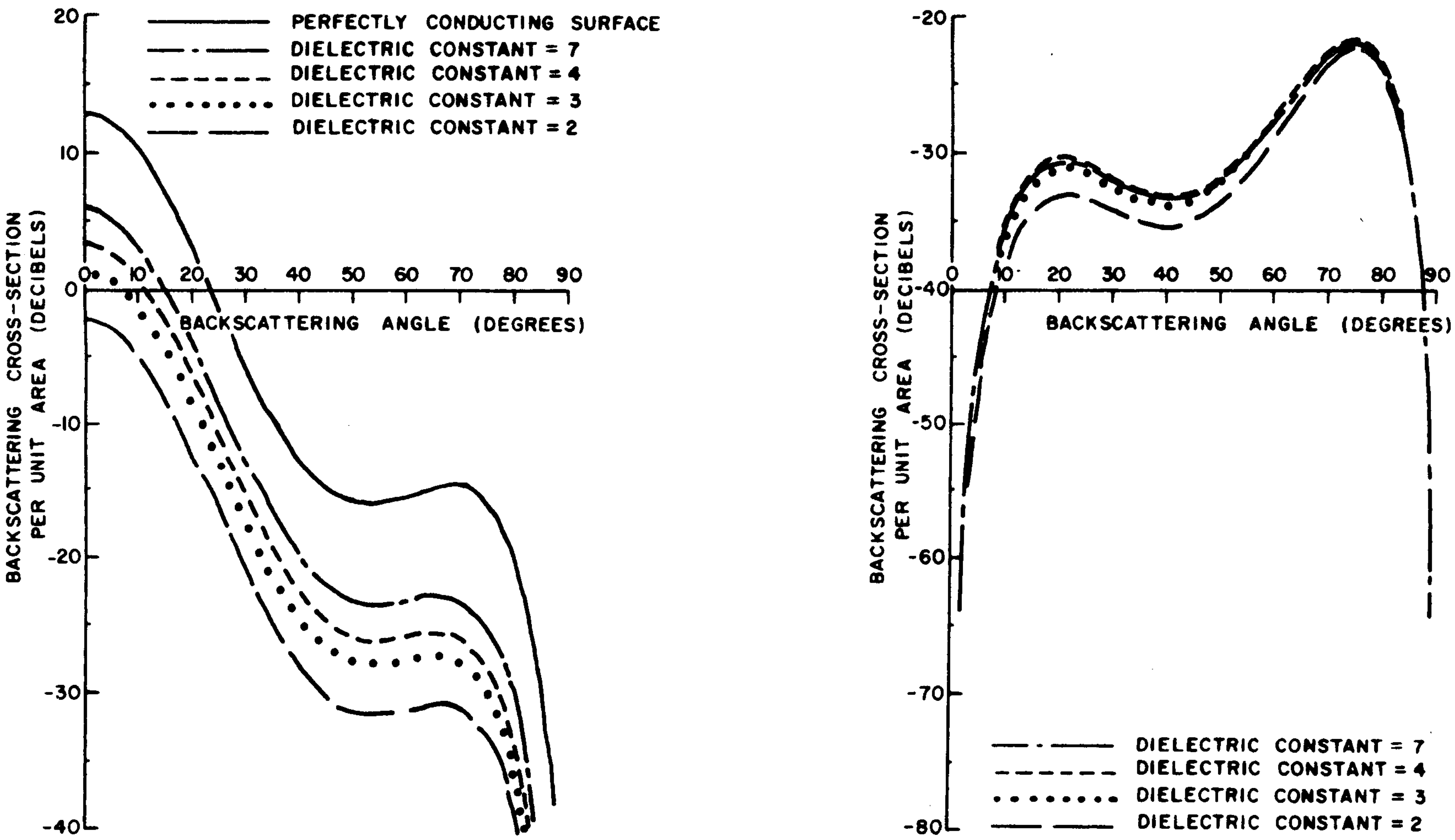

(a) Polarized backscattered component.

(b) Depolarized backscattered component.

Fig. E-5--Predicted backscattering cross sections for a rough planar surface using circular polarization. RMS surface slope = 12.5°. Gaussian JPDF for surface height.

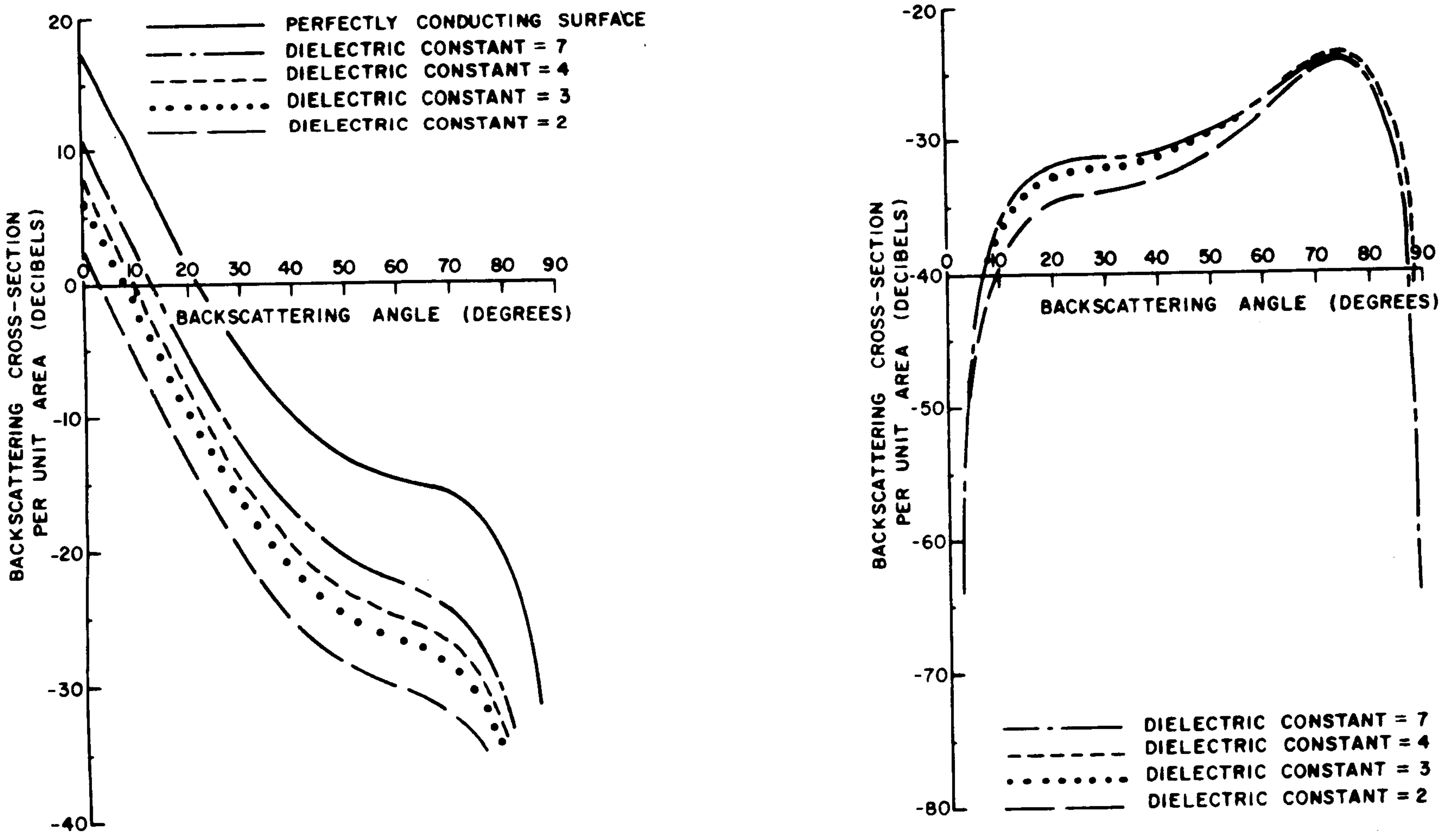

(a) Polarized backscattered component.

(b) Depolarized backscattered component.

Fig. E-6--Predicted backscattering cross sections for a rough planar surface using circular polarization. RMS surface slope = 12.5°. Bessel JPDF for surface height.

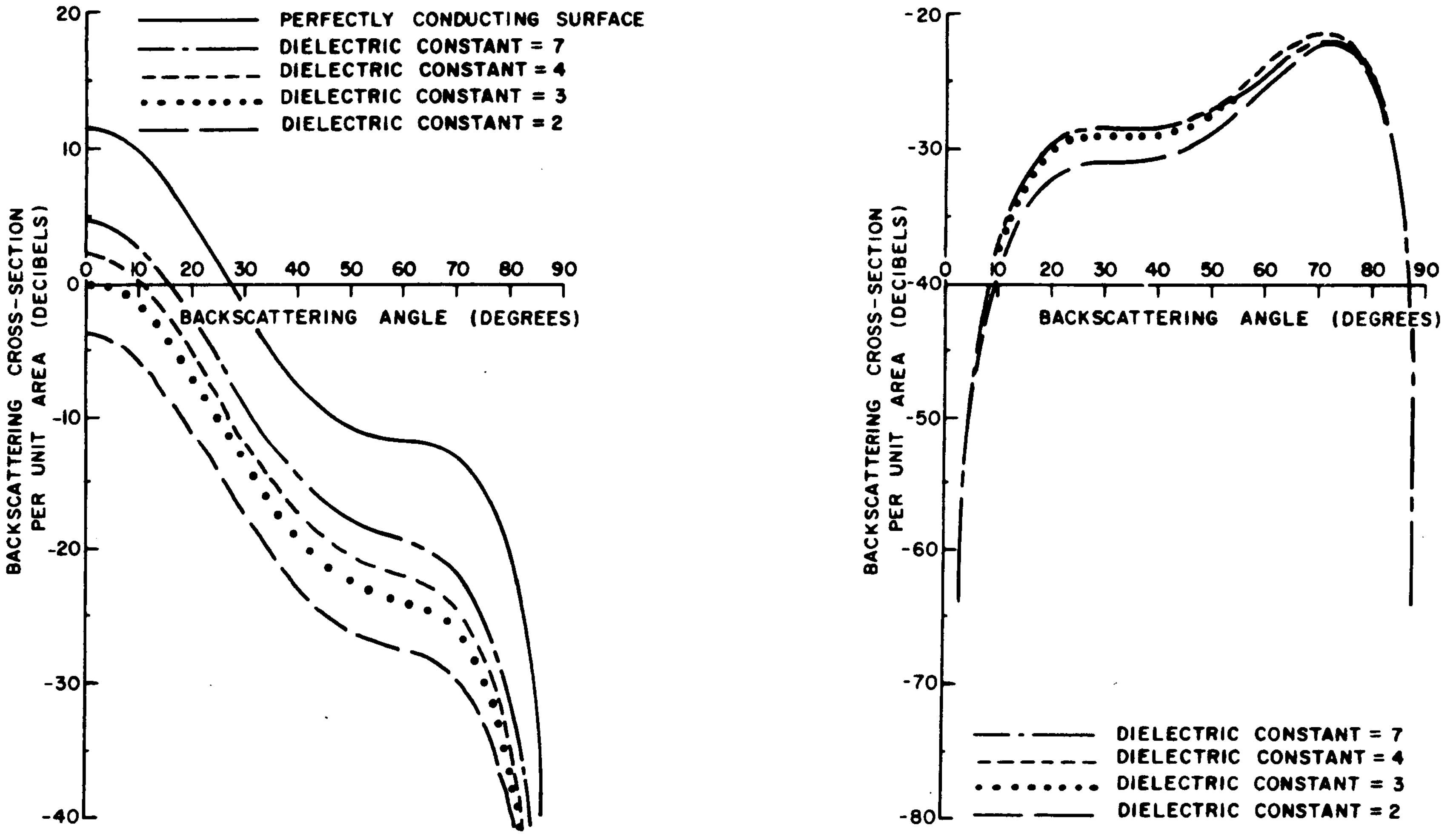

(a) Polarized backscattered component.

(b) Depolarized backscattered component.

Fig. E-7--Predicted backscattering cross sections for a rough planar surface using circular polarization. RMS surface slope = 15°. Gaussian JPDF for surface height.

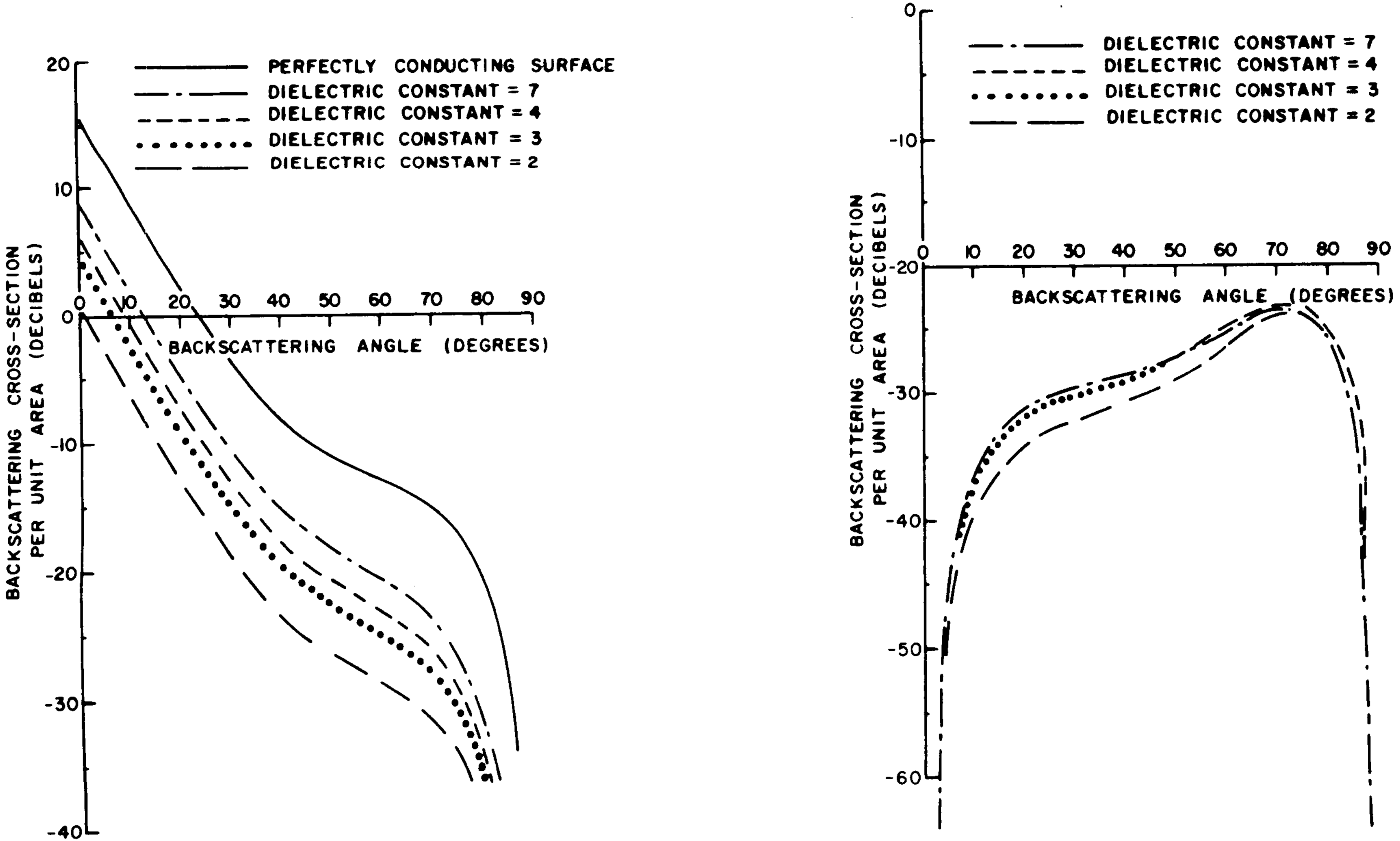

(a) Polarized backscattered component.

(b) Depolarized backscattered component.

Fig. E-8--Predicted backscattering cross sections for a rough planar surface using circular polarization. RMS surface slope = 15°. Bessel JPDF for surface height.

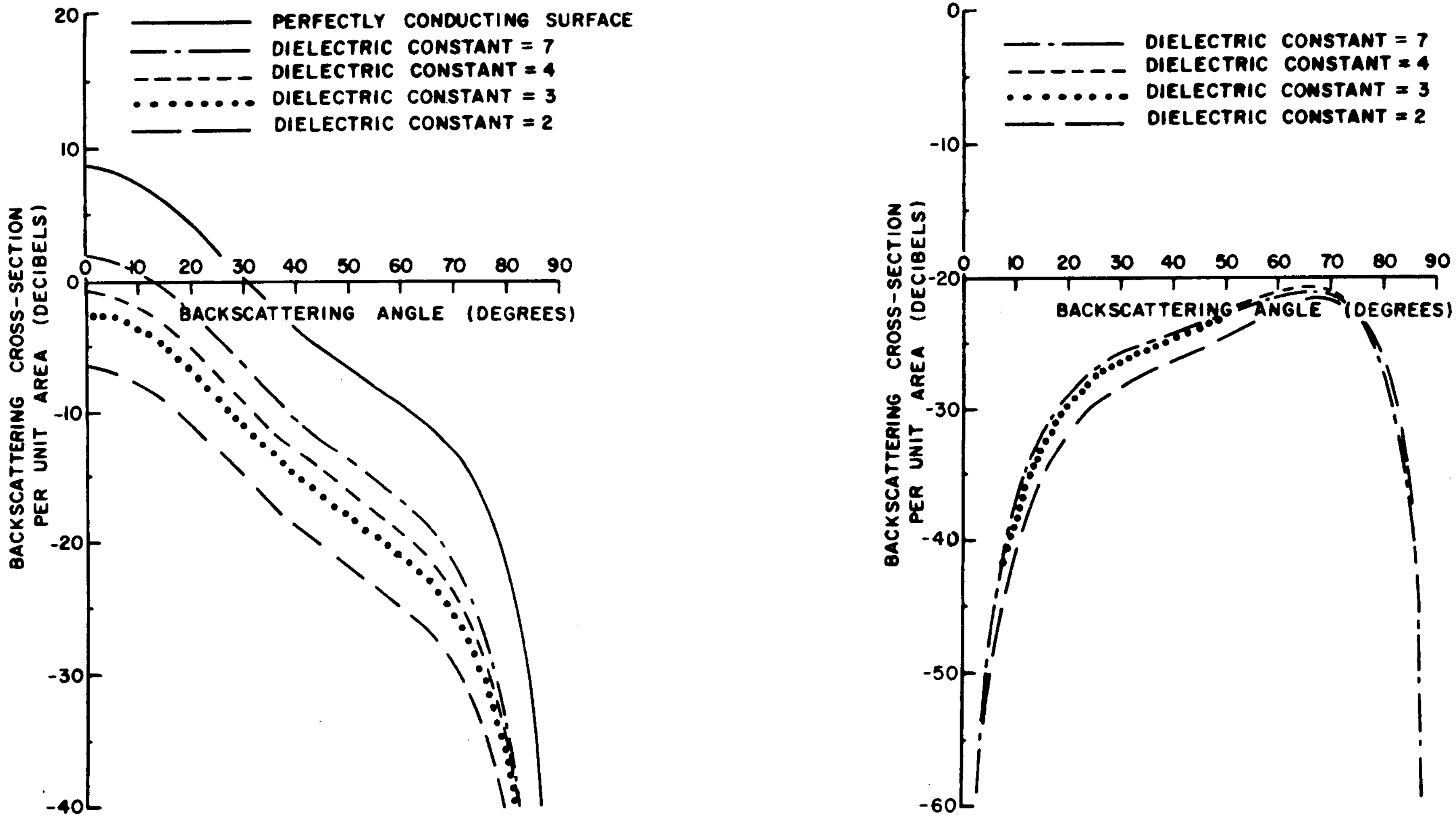

(a) Polarized backscattered component.

(b) Depolarized backscattered component.

Fig. E-9--Predicted backscattering cross sections for a rough planar surface using circular polarization. RMS surface slope = 20°. Gaussian JPDF for surface height.

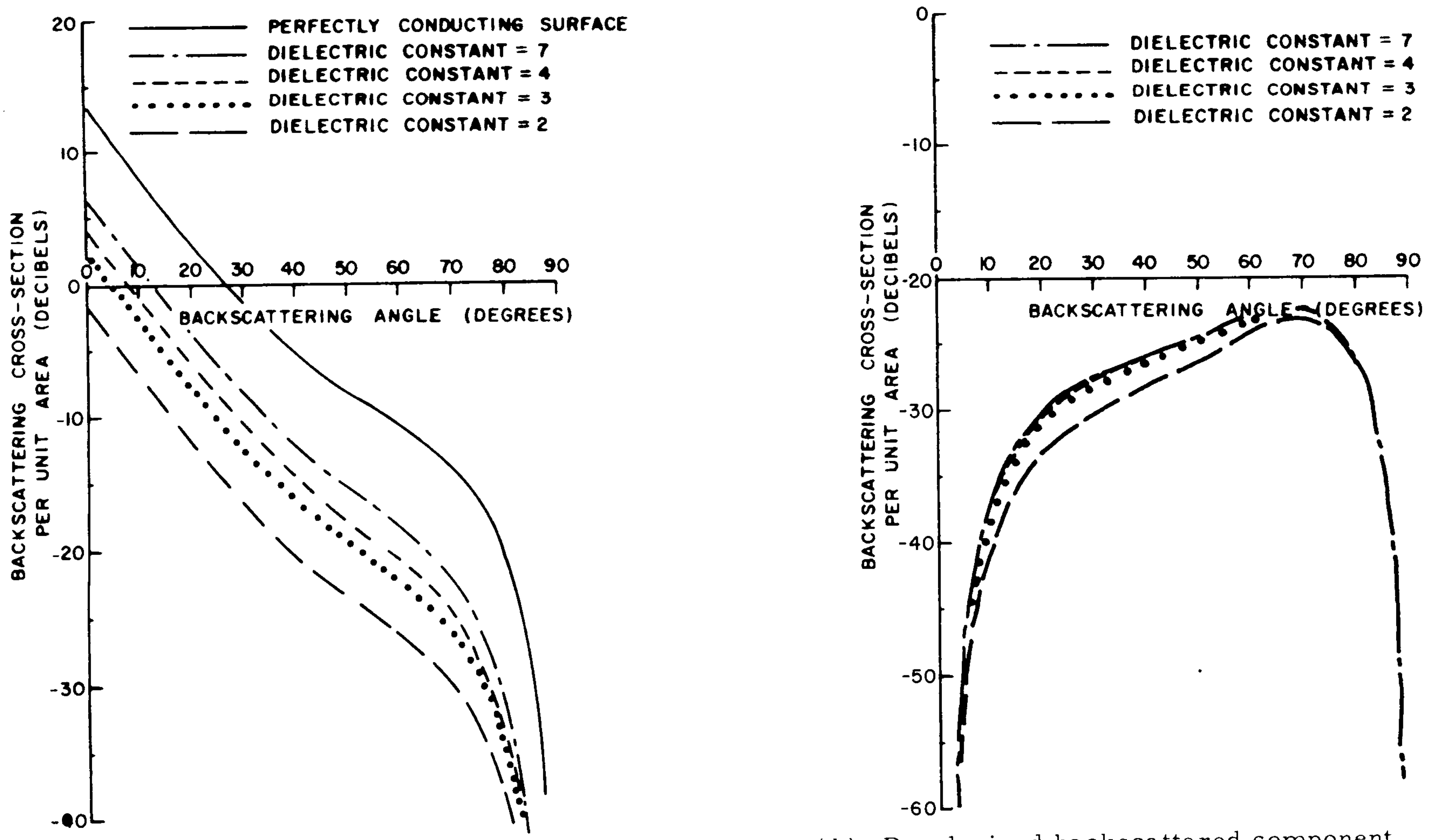

(a) Polarized backscattered component.

(b) Depolarized backscattered component.

Fig. E-10--Predicted backscattering cross sections for a rough planar surface using circular polarization. RMS surface slope = 20°. Bessel JPDF for surface height.

SECTION F

The predicted curves for backscattering cross section per unit area of a rough planar surface are shown when only linearly polarized waves are transmitted and received. It can be seen that a difference in return exists between transmitting vertical-receiving vertical and transmitting horizontal-receiving horizontal in the case of dielectric surfaces; in the case of a perfectly conducting surface, however, the returns are identical because such a surface has been shown to be polarization-blind. This difference in return between the vertical-vertical and horizontal-horizontal cross sections for dielectric surfaces incorporates the Brewster angle effect present in the vertical-vertical case. The magnitude of this Brewster angle effect and the value of the Brewster angle itself are functions of surface roughness and dielectric constant. The magnitude of the Brewster angle effect diminishes as surface roughness increases, as can be seen by comparing the returns for rms surface slopes of 15° and 20° .

The depolarized or cross polarized component in the backscattered field is present in the return from non-perfectly conducting surfaces. It is the same (evident from reciprocity considerations) for the case of horizontal transmitting-vertical receiving as for the case of vertical transmitting-horizontal receiving.

The curves in this section are plotted from equations (3. 10a) and (3. 10c) of Report 1388-18 for the perfectly conducting surfaces and from equations (3. 18 a, b, and c) for the lossy dielectric surfaces.

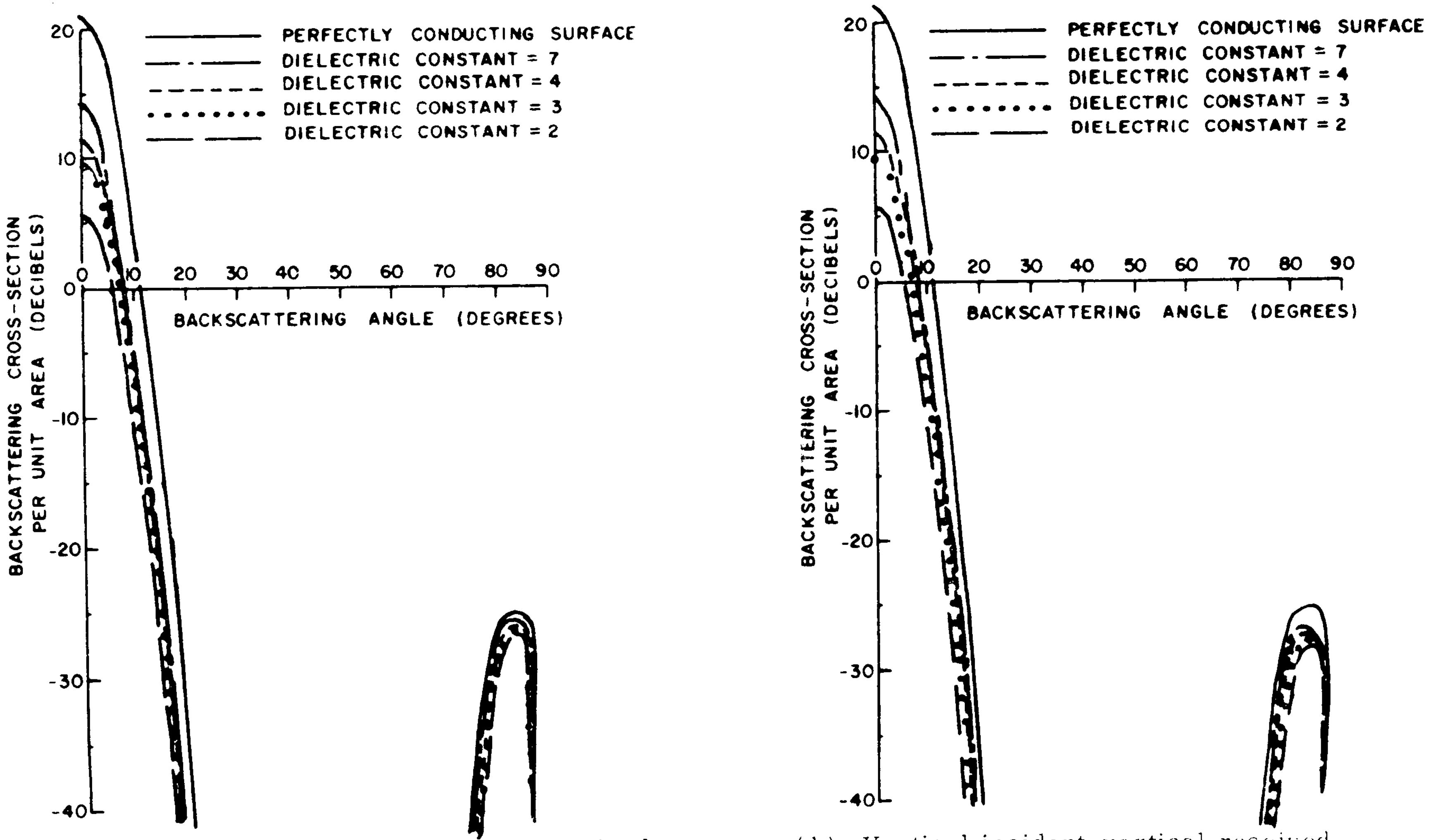

(a) Horizontal incident-horizontal received

(b) Vertical incident-vertical received

Fig. F-1.

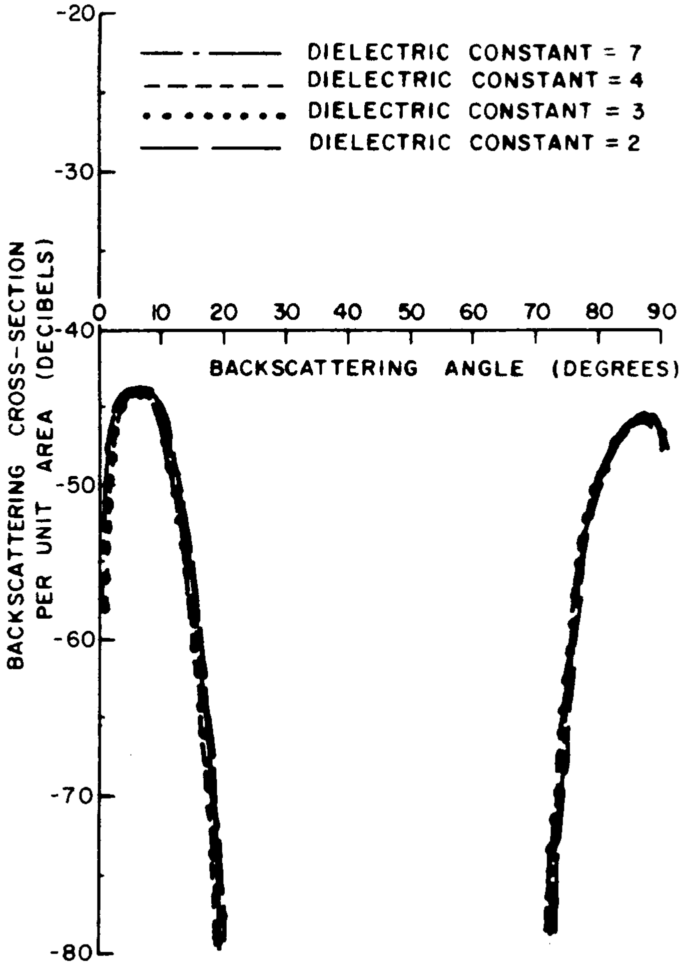

(c) Horizontal/vertical incident - vertical/horizontal received

Fig. F-1--Predicted backscattering cross sections for a rough planar surface using linear polarization. RMS surface slope = 5°. Gaussian JPDF for surface height.

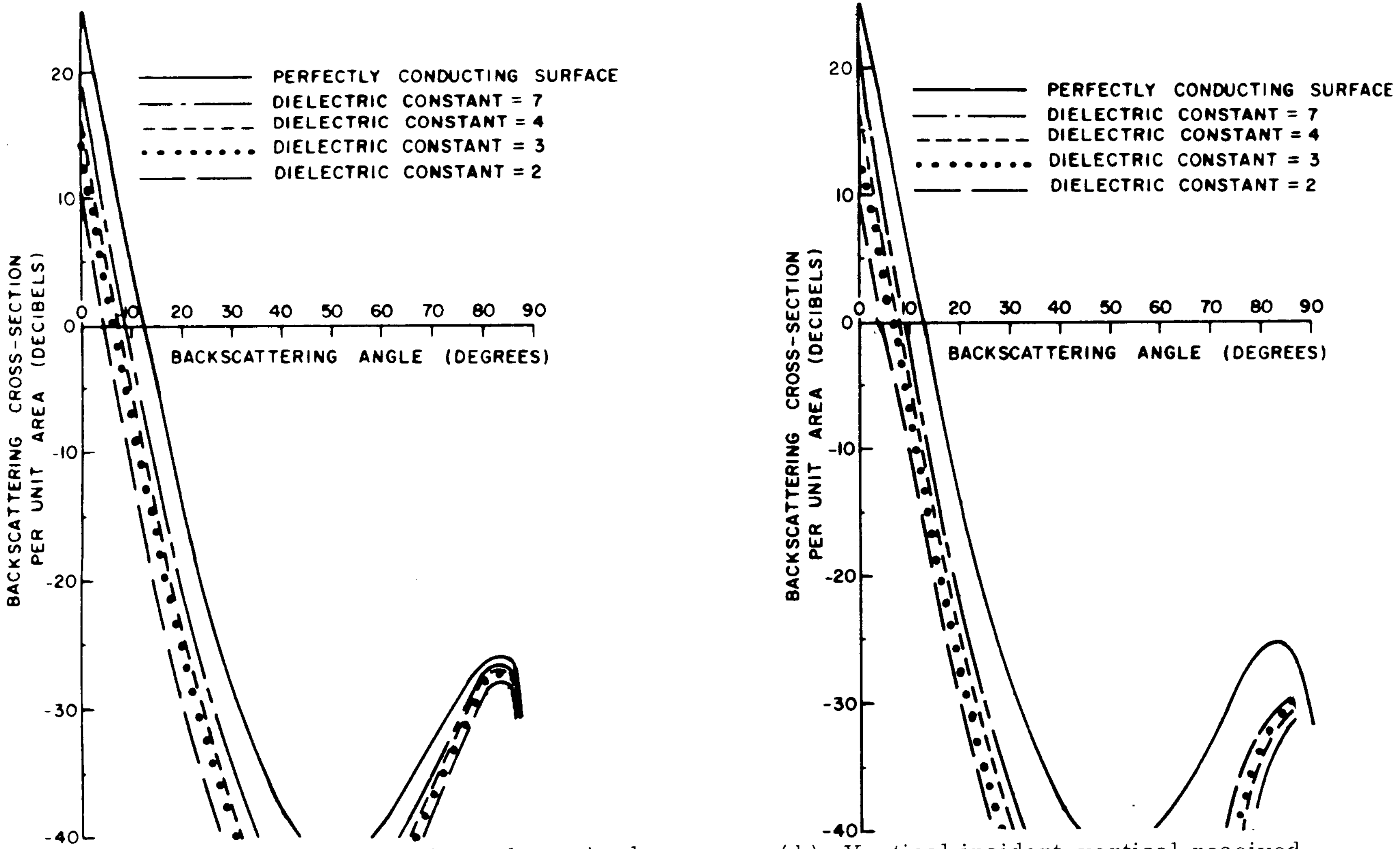

(a) Horizontal incident-horizontal received

(b) Vertical incident-vertical received

Fig. F-2.

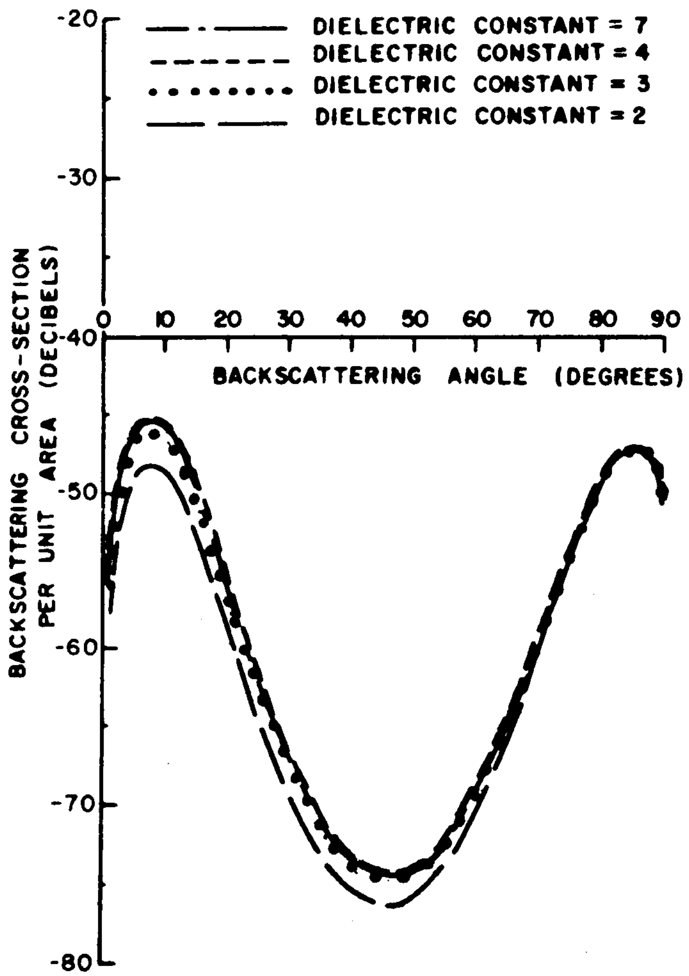

(c) Horizontal/vertical incident-vertical/horizontal received.

Fig. F-2--Predicted backscattering cross sections for a rough planar surface using linear polarization. RMS surface slope = 5°. Bessel JPDF for surface height.

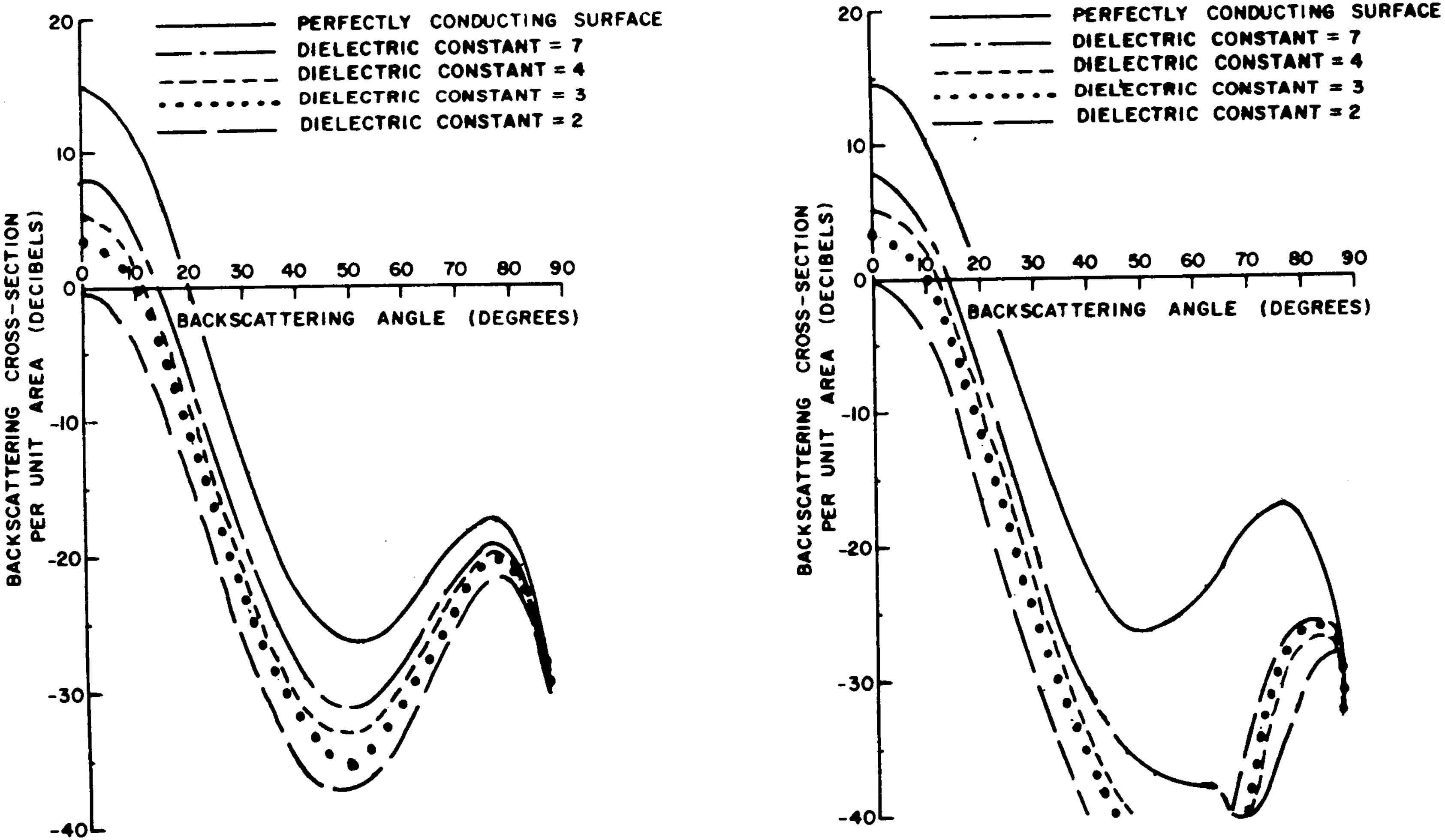

(a) Horizontal incident-horizontal received

(b) Vertical incident-vertical received.

Fig. F-3.

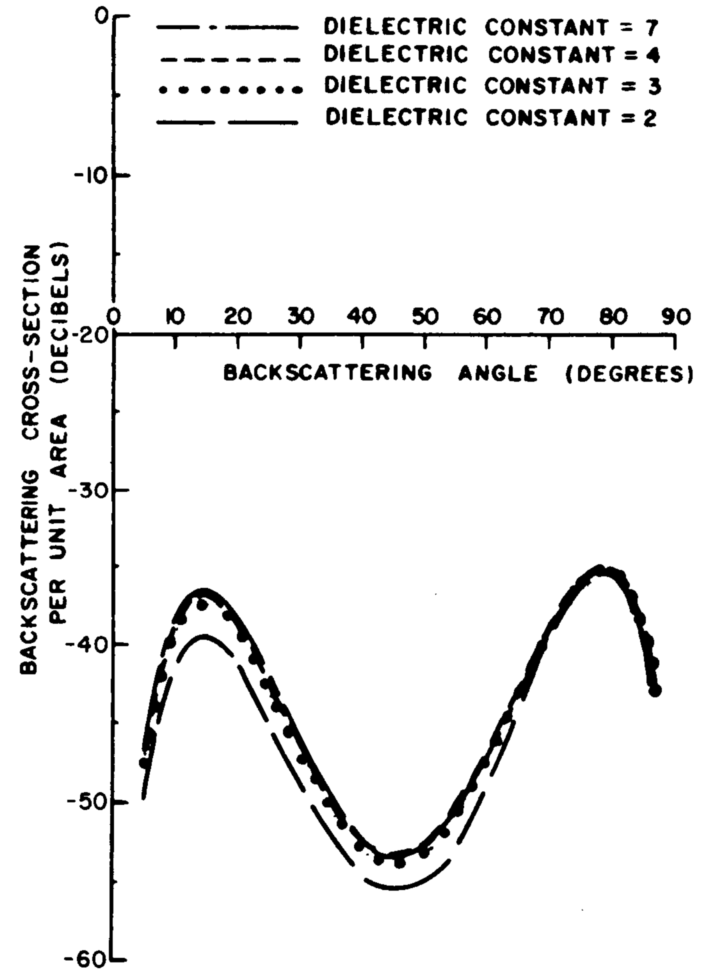

(c) Horizontal/vertical incident-vertical/horizontal received.

Fig. F-3--Predicted backscattering cross sections for a rough planar surface using linear polarization. RMS surface slope = 10°. Gaussian JPDF for surface height.

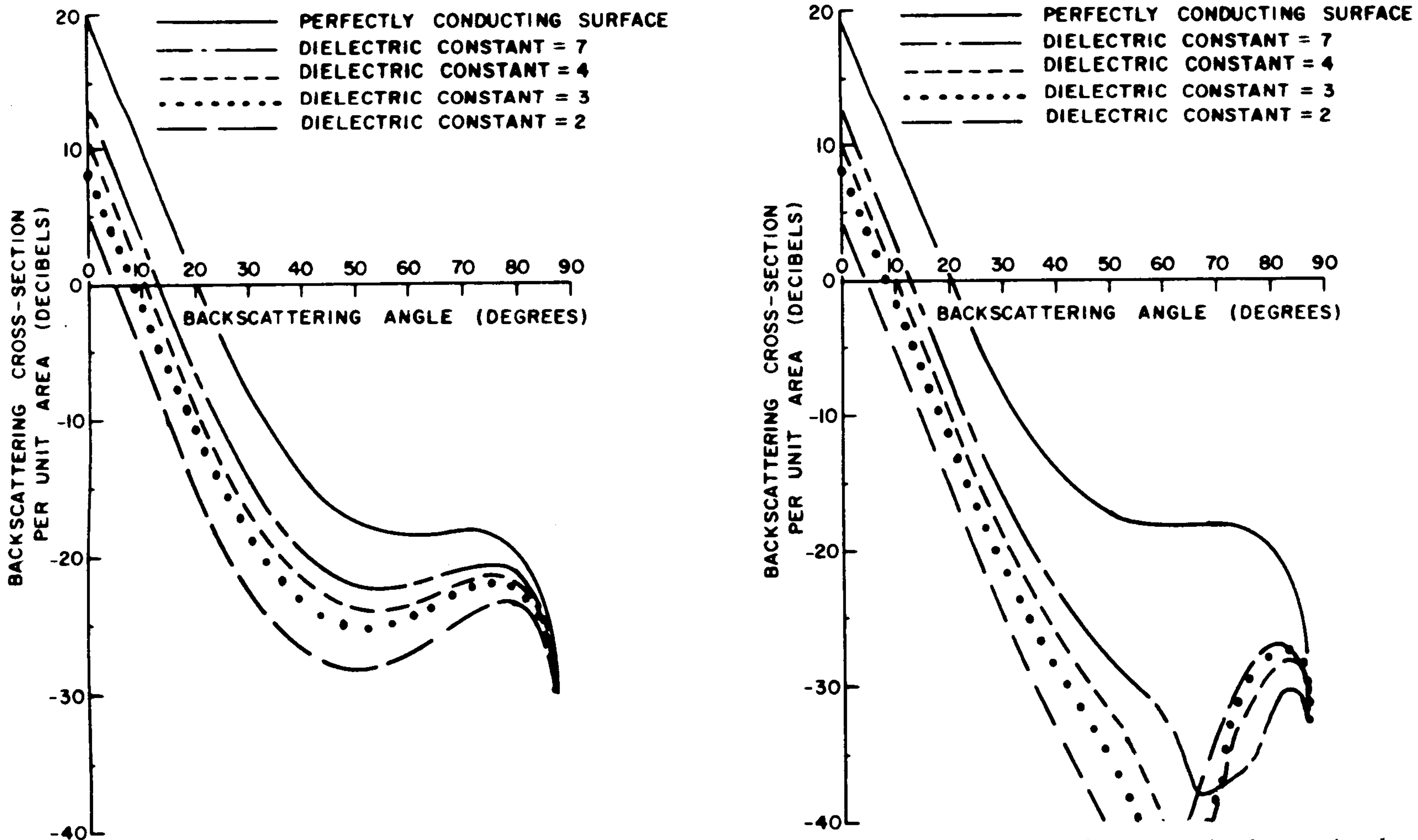

(a) Horizontal incident-horizontal received.

(b) Vertical incident-vertical received.

Fig. F-4.

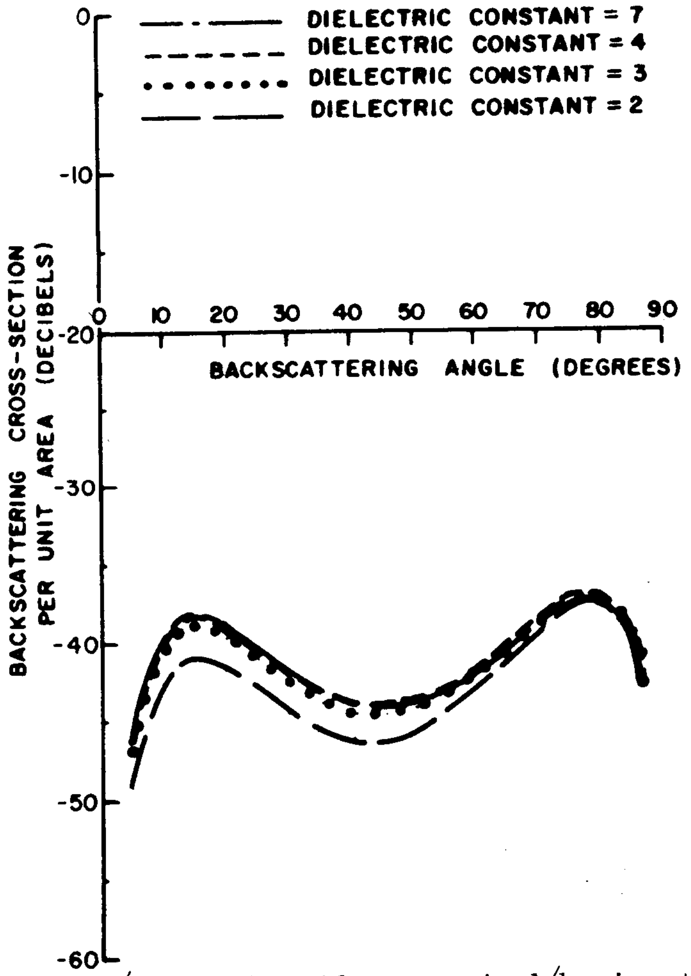

(c) Horizontal/vertical incident-vertical/horizontal received.

Fig. F-4--Predicted backscattering cross sections for a rough planar surface using linear polarization. RMS surface slope =10°. Bessel JPDF for surface height.

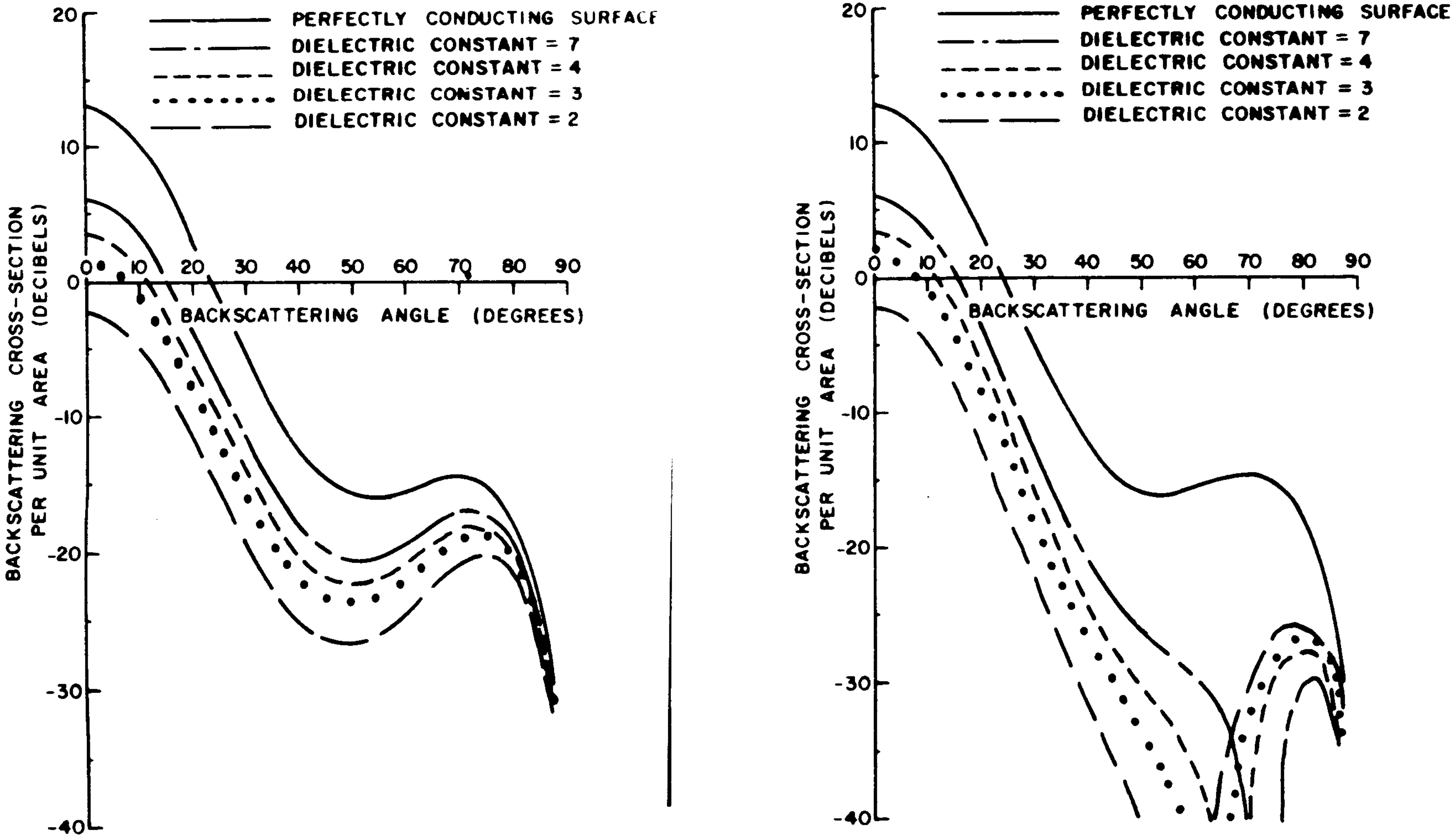

(a) Horizontal incident-horizontal received.

(b) Vertical incident-vertical received.

Fig. F-5.

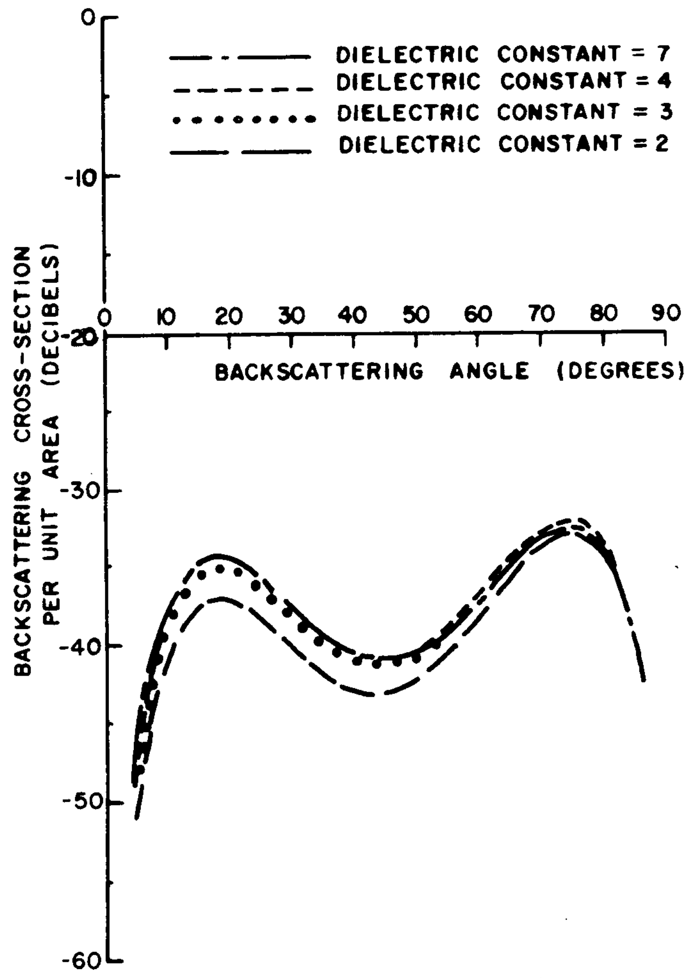

(c) Horizontal/vertical incident-vertical/horizontal received.

Fig. F-5--Predicted backscattering cross sections for a rough planar surface using linear polarization. RMS surface slope = 12. 5°. Gaussian JPDF for surface height.

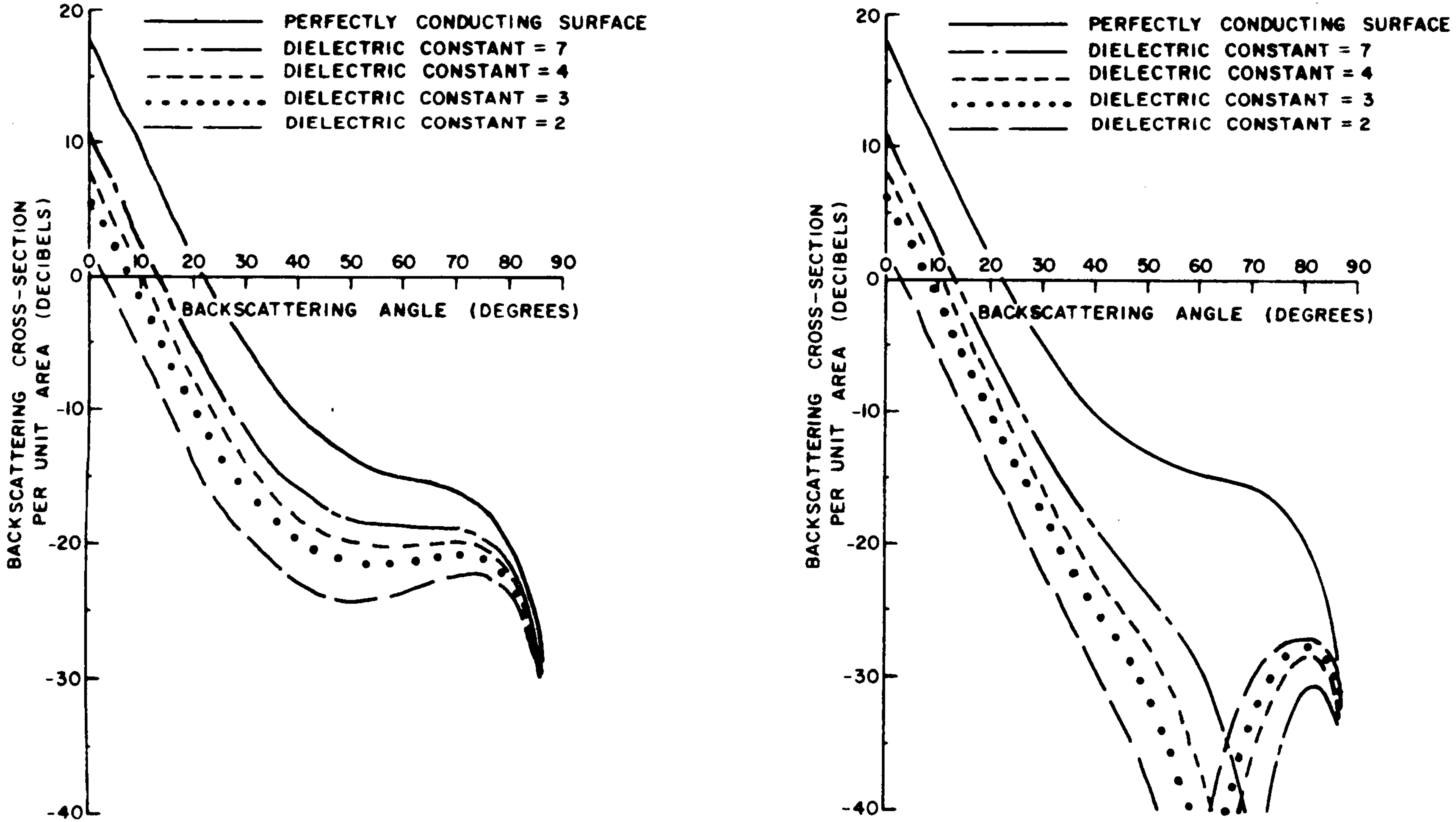

(a) Horizontal incident-horizontal received.

(b) Vertical incident-vertical received.

Fig. F-6.

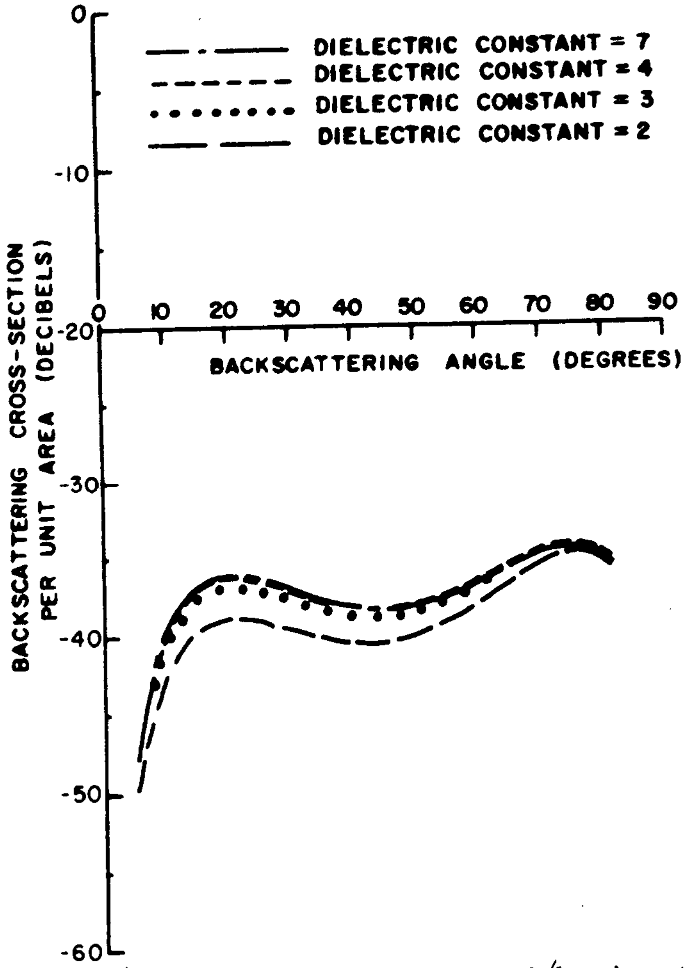

(c) Horizontal/vertical incident-vertical/horizontal received.

Fig. F-6--Predicted backscattering cross sections for a rough planar surface using linear polarization. RMS surface slope = 12. 5°. Bessel JPDF for surface height.

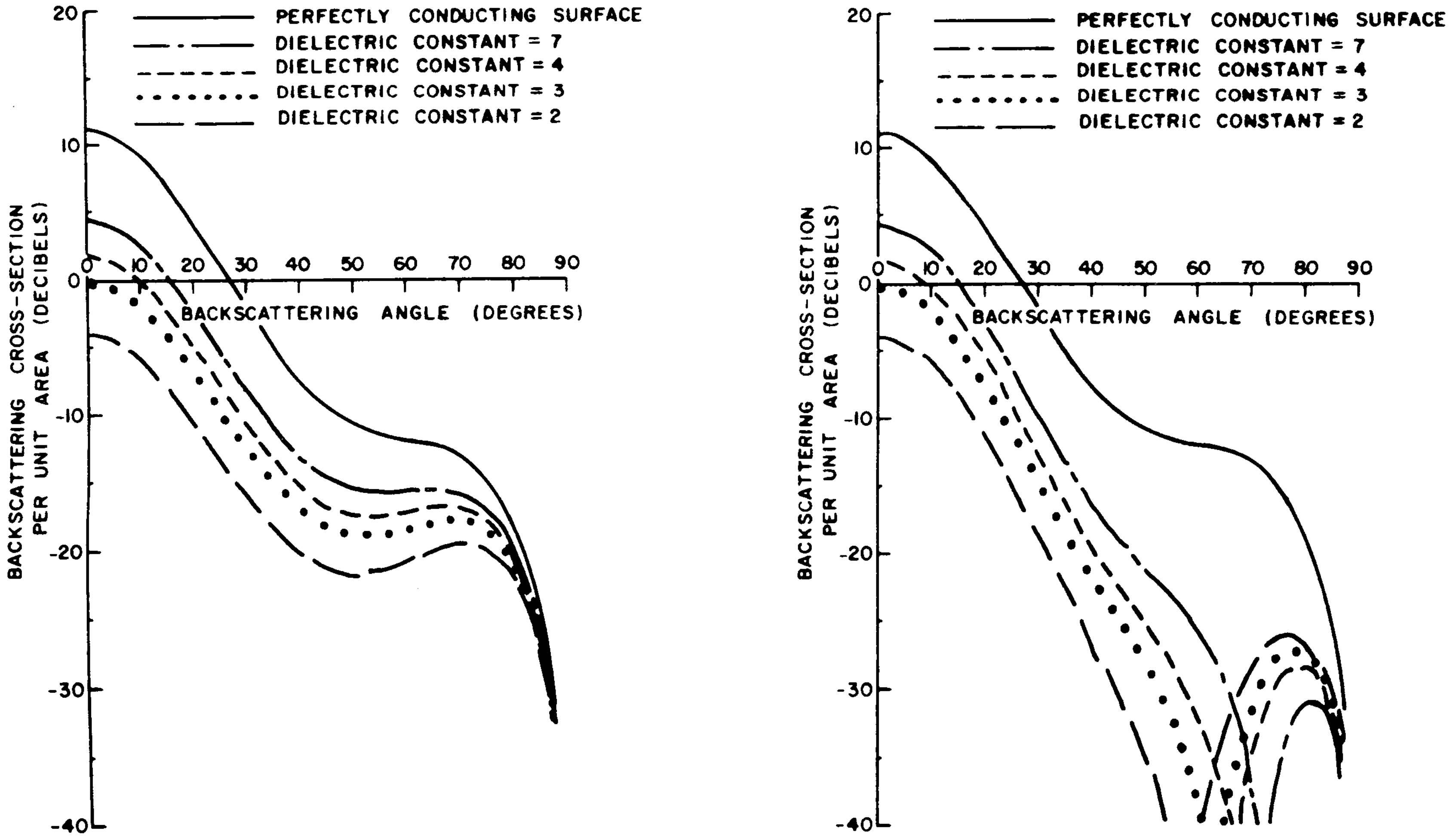

(a) Horizontal incident-horizontal received.

(b) Vertical incident-vertical received.

Fig. F-7.

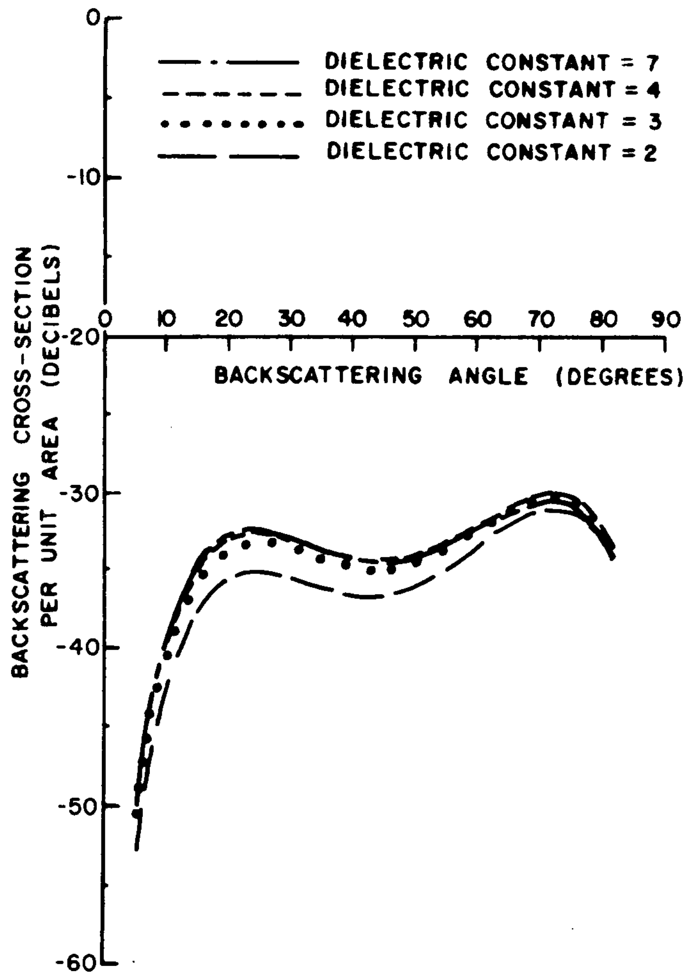

(c) Horizontal/vertical incident-vertical/horizontal received.

Fig. F-7--Predicted backscattering cross sections for a rough planar surface using linear polarization. RMS surface slope = 15°. Gaussian JPDF for surface height.

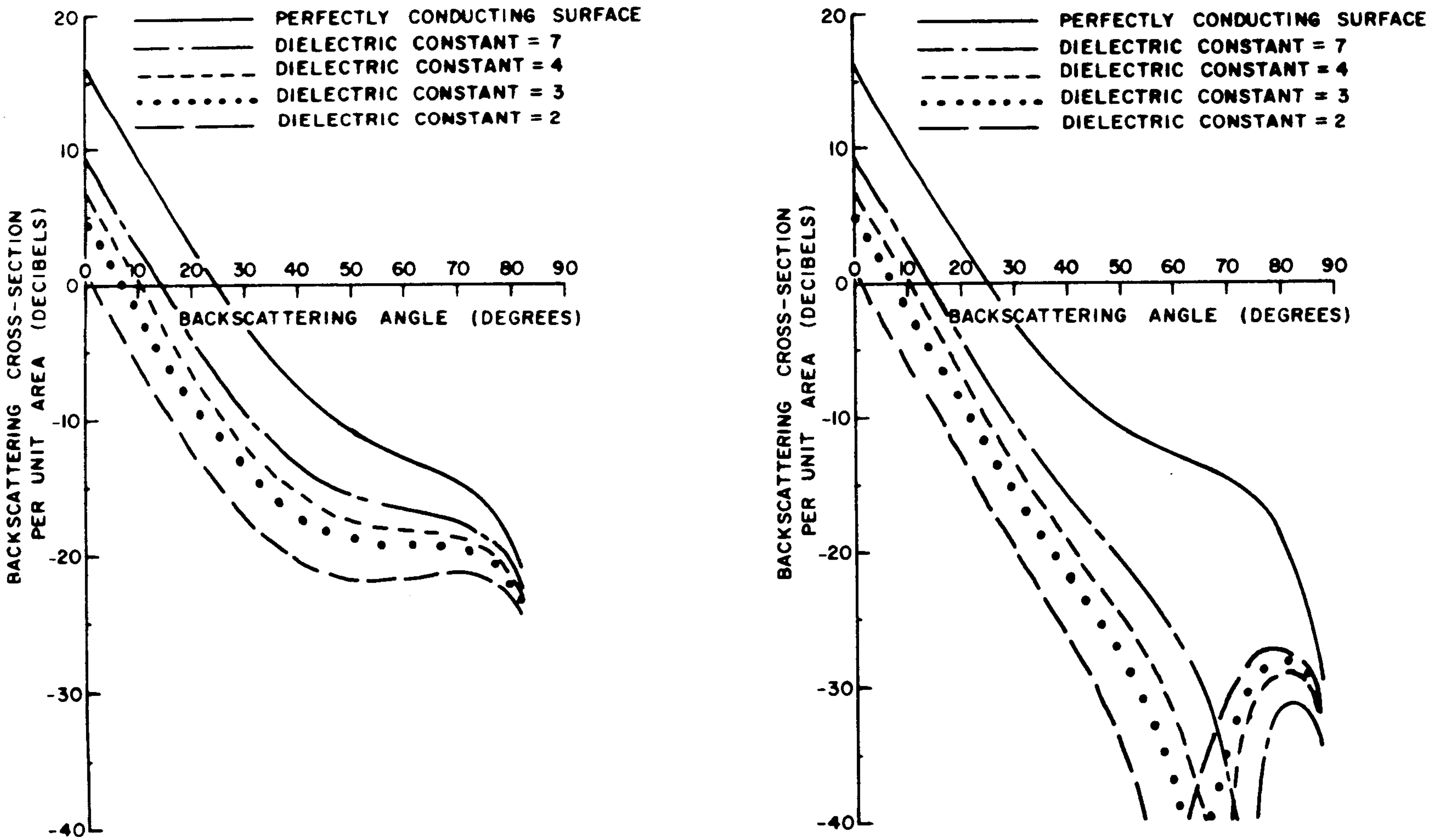

(a) Horizontal incident-horizontal received.

(b) Vertical incident-vertical received.

Fig. F-8.

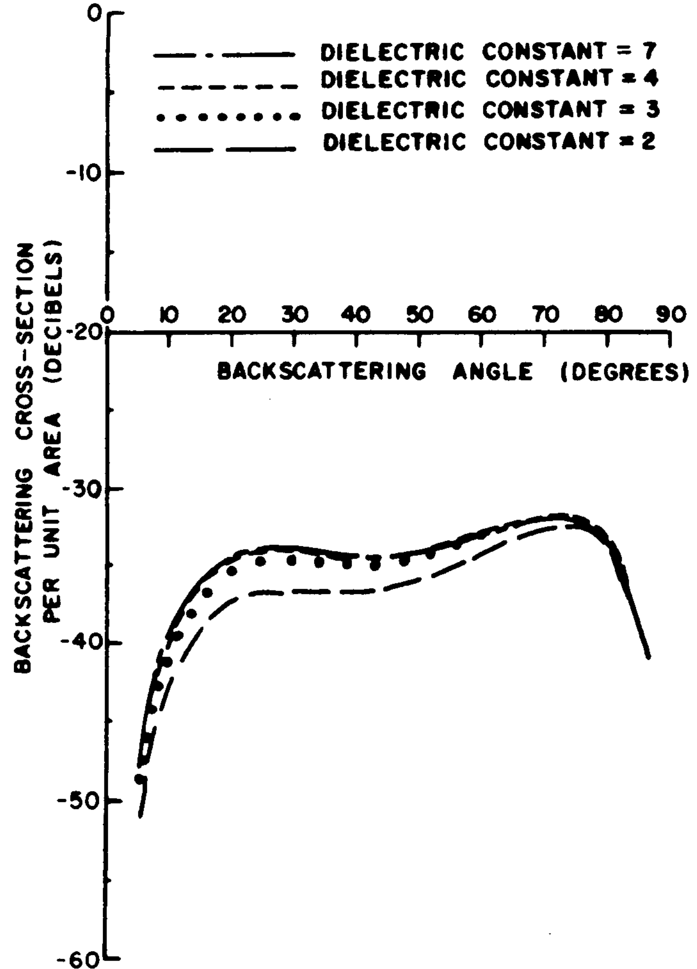

(c) Horizontal/vertical incident-vertical/horizontal received.

Fig. F-8--Predicted backscattering cross sections for a rough planar surface using linear polarization. RMS surface slope = 15°. Bessel JPDF for surface height.

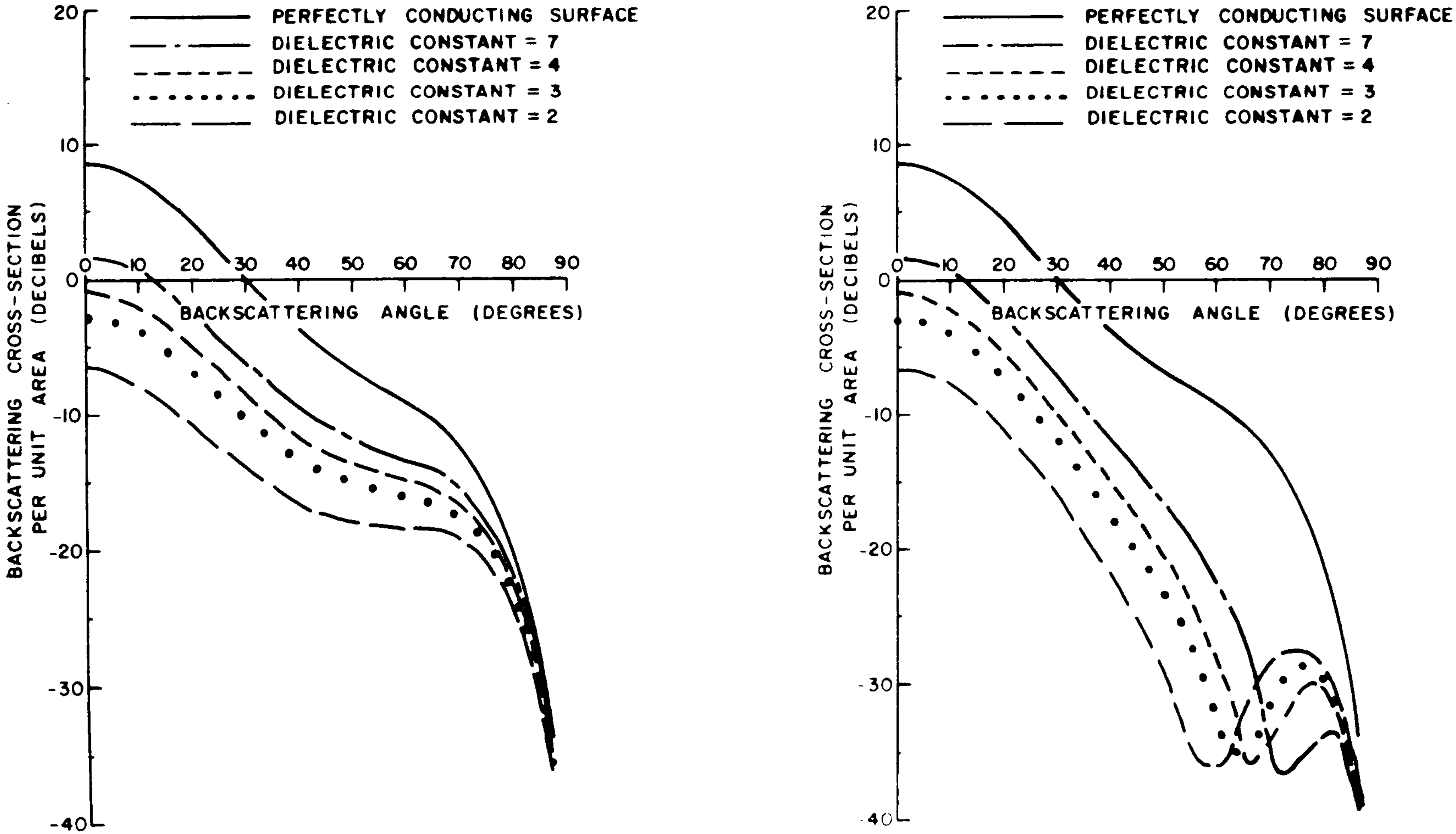

(a) Horizontal incident-horizontal received.

(b) Vertical incident-vertical received.

Fig. F-9.

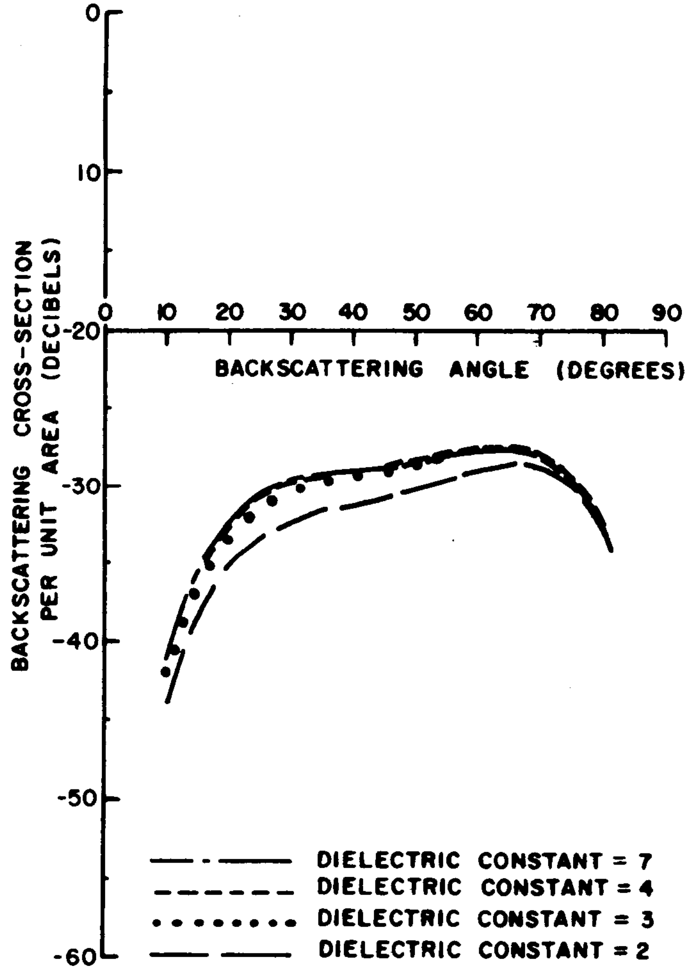

(c) Horizontal/vertical incident-vertical/horizontal received.

Fig. F-9--Predicted backscattering cross sections for a rough planar surface using linear polarization. RMS surface slope = 20°. Gaussian JPDF for surface height.

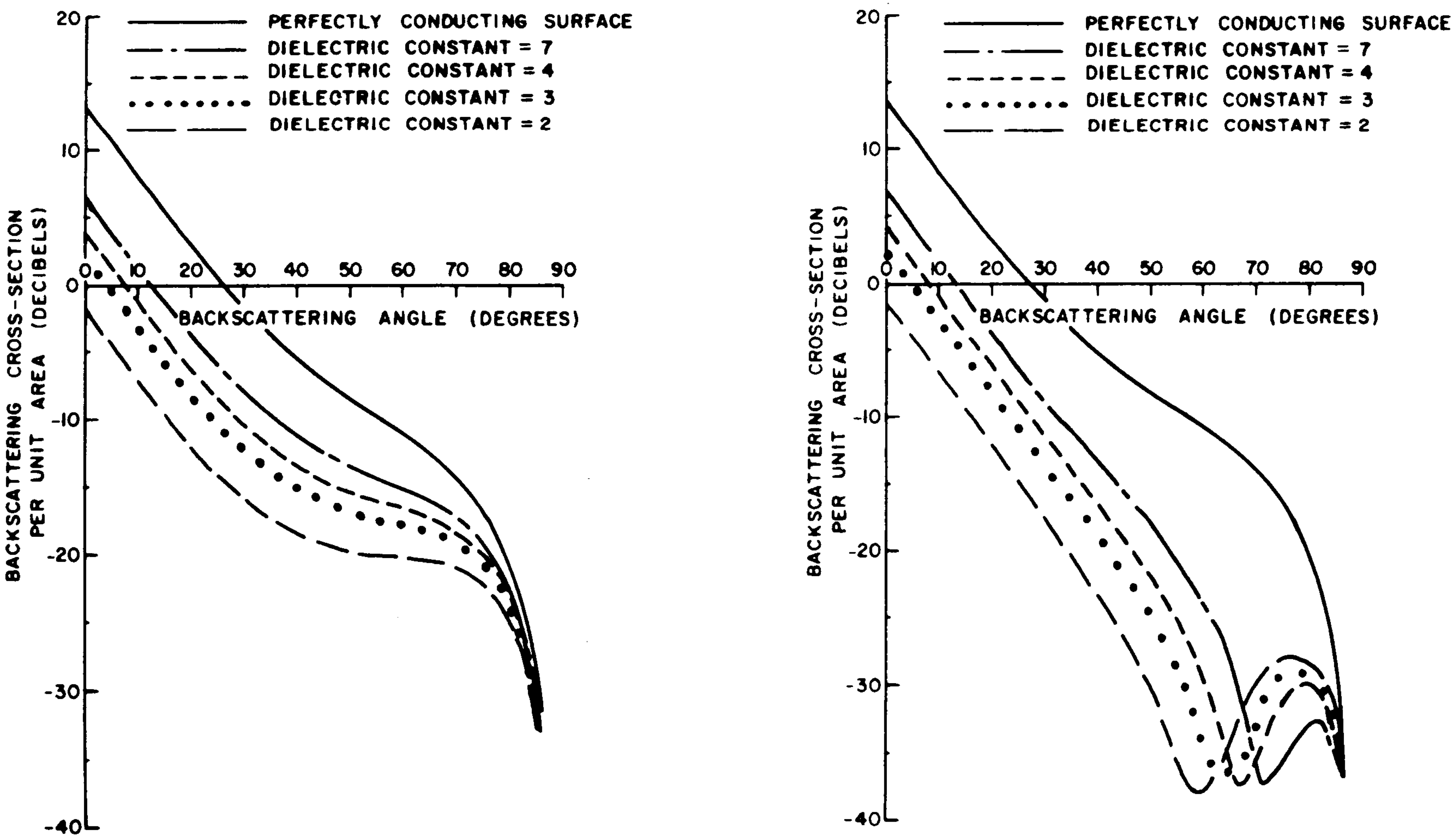

(a) Horizontal incident-horizontal received.

(b) Vertical incident-vertical received.

Fig. F-10.

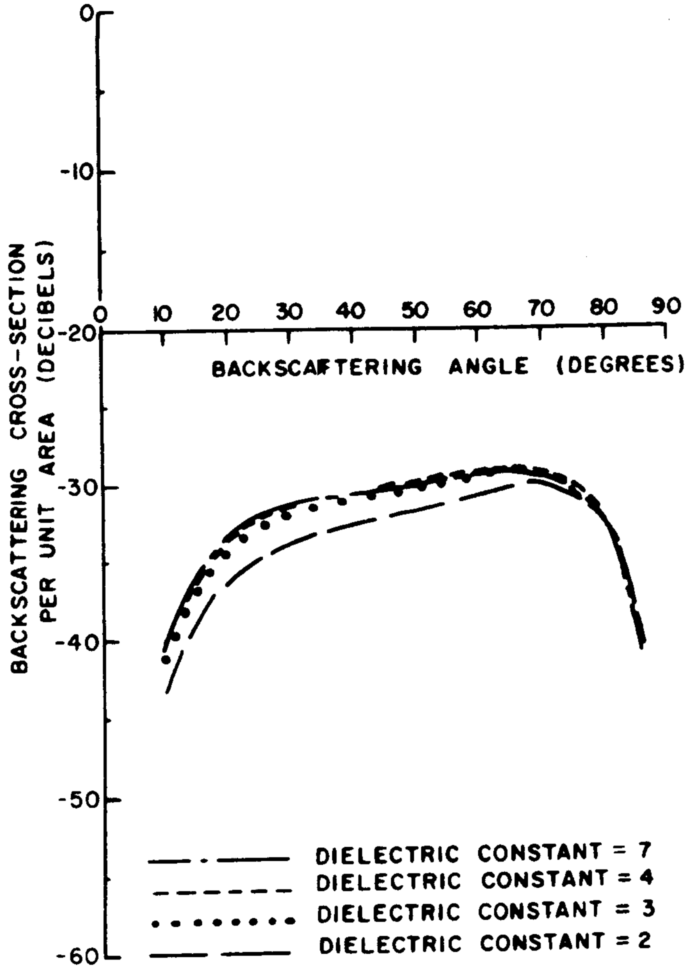

(c) Horizontal/vertical incident-vertical/horizontal received.

Fig. F-10--Predicted backscattering cross sections for a rough planar surface using linear polarization. RMS surface slope = 20°. Bessel JPDF for surface height.

SECTION G

The predicted curves for backscattering cross section per unit area of a rough annular surface section of a sphere illuminated by a pulse when linearly polarized waves are transmitted and received are plotted in this section (see Fig. G-1). One must deal with such a situation when he attempts to analyze the backscattering cross section of the moon or planets as a function of time when narrow (compared to the radius) radar pulses are transmitted.

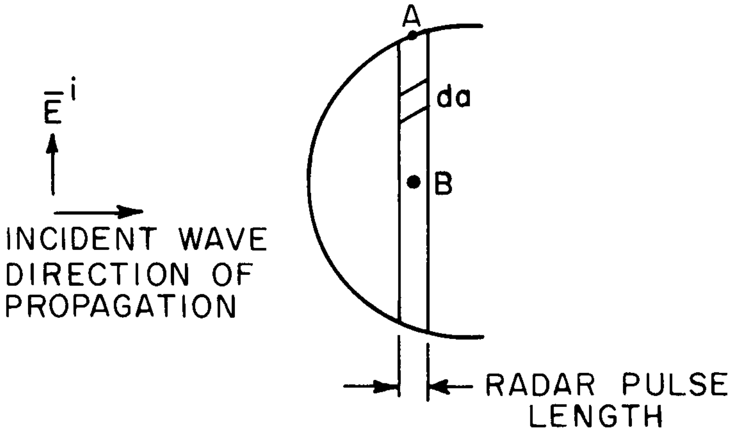

Fig. G-1. Geometry of spherical scattering body illuminated by a radar pulse.

It can be seen from the geometry of such an annular section that one can no longer refer to an incident wave as being only vertically or horizontally polarized with respect to the illuminated area; rather, the wave is vertically polarized at two points on the ring, horizontally polarized at two points 90° away from the vertical points, and obliquely polarized at all other points. Therefore, when one transmits and receives linearly polarized waves, he must average the contribution from each point of the ring in terms of vertically and horizontally polarized waves at that point over the entire ring. This analysis was carried out in detail in Report 1388-17, and the results were used in Report 1388-18 to predict the backscattering cross section for such a range ring for the two statistical models considered.

It should be noted that such an analysis is not necessary when one is transmitting and receiving circularly polarized waves. A right circularly polarized incident wave, for example, is right circular at every point on the illuminated ring. Therefore, the curves of Section E may be used as they are for this pulse illumination of a rough spherical surface.

Two polarization situations are treated in this section. The first curve of every page represents the situation where the transmitting and receiving antennas are linearly polarized along the same direction. The second curve shows the predicted result when the direction of linear polarization of transmitting and receiving antennas are 90° apart; this curve therefore represents the depolarized power in the backscattering direction.

The curves are plotted from equations (3.10a) and (3.10c) of Report 1388-18 for the perfectly conducting surface and from equations (3.20a) and (3.20b) for the lossy dielectric surfaces.

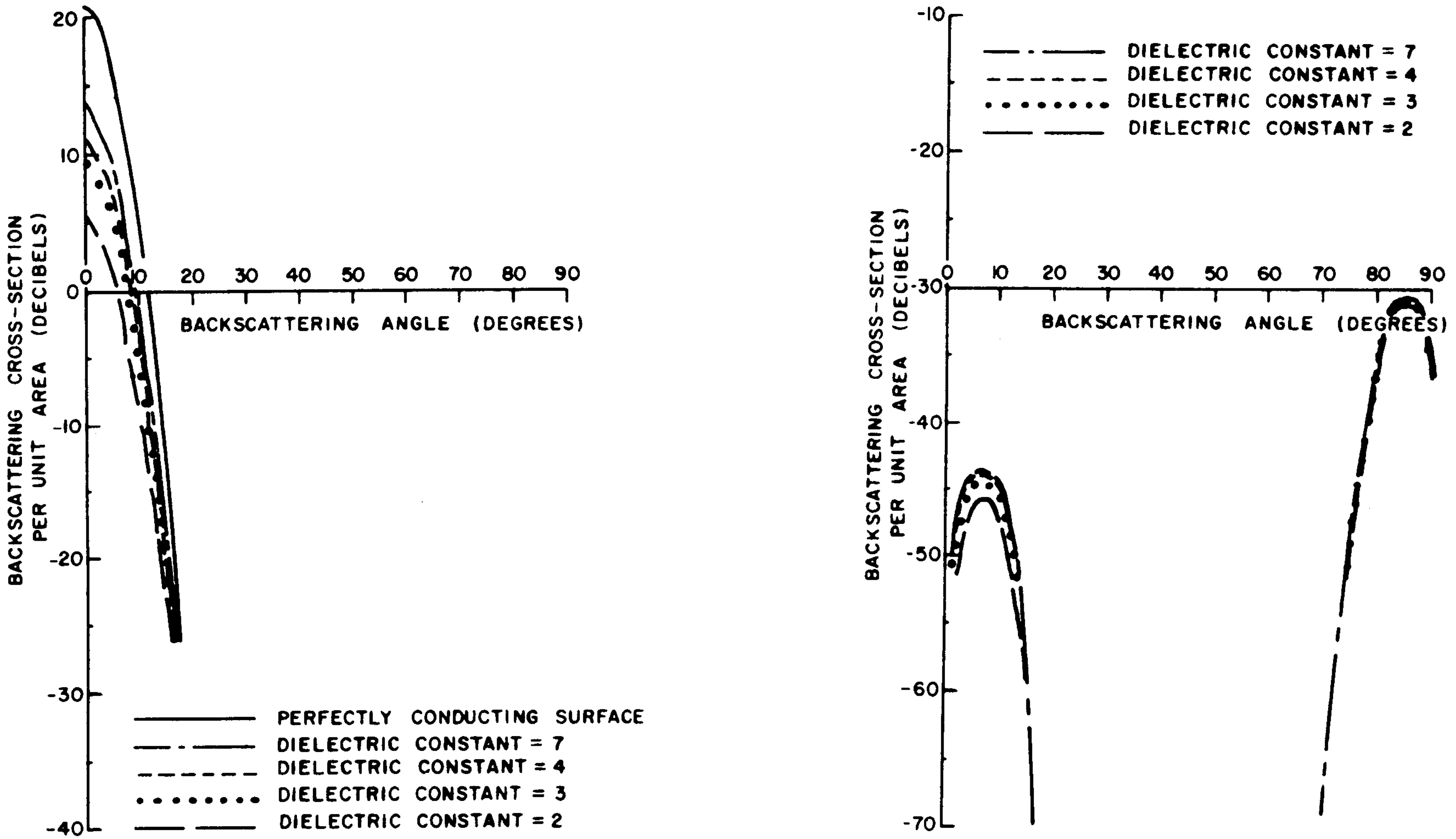

(a) Transmitting and receiving polarizations parallel.

(b) Transmitting and receiving polarizations perpendicular.

Fig. G-1--Predicted backscattering cross section for a pulse-illuminated planetary range ring using linear polarization. RMS surface slope = 5°. Gaussian JPDF for surface height.

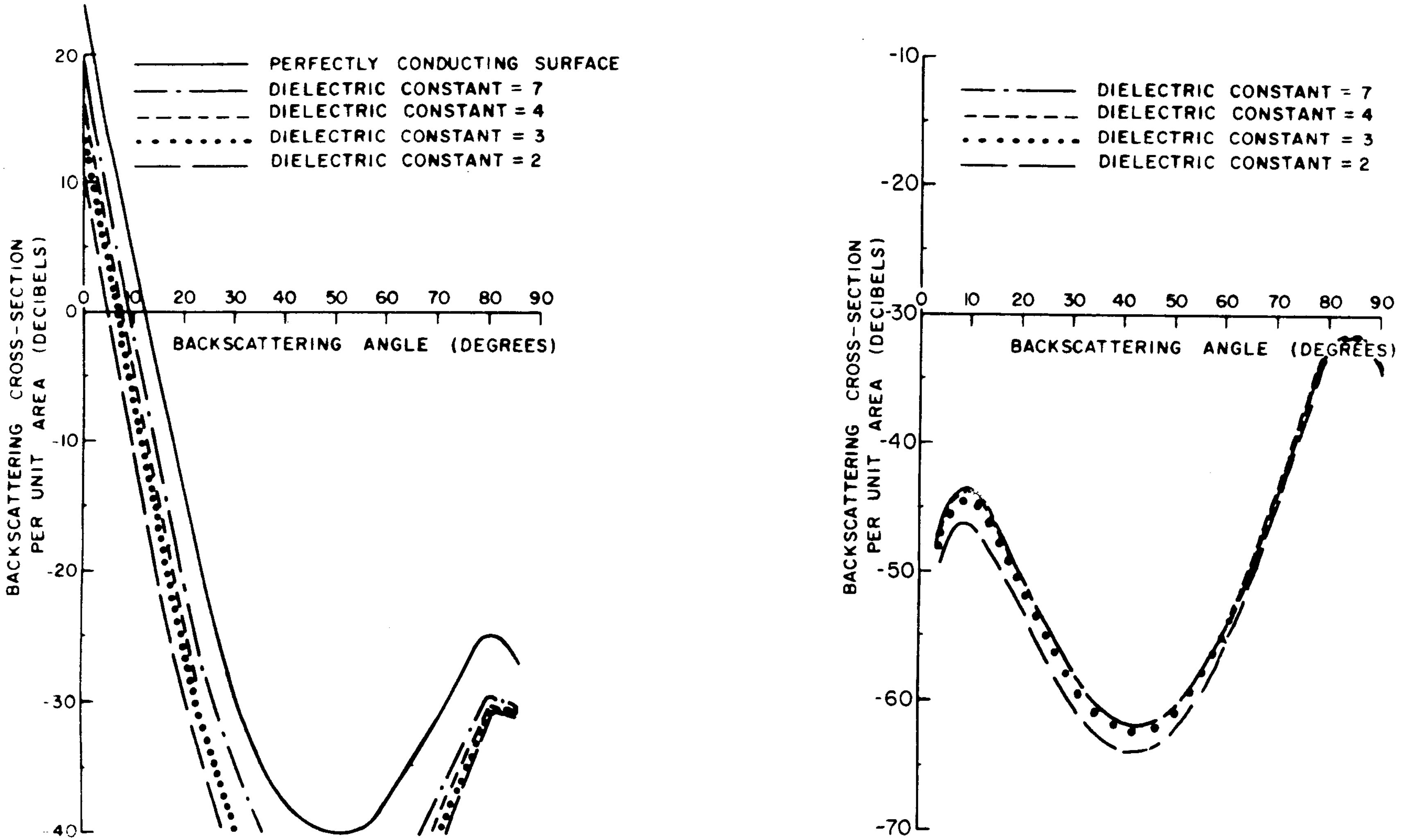

(a) Transmitting and receiving polarizations parallel.

(b) Transmitting and receiving polarizations perpendicular.

Fig. G-2--Predicted backscattering cross section for a pulse-illuminated planetary range ring using linear polarization. RMS surface slope = 5°. Bessel JPDF for surface height.

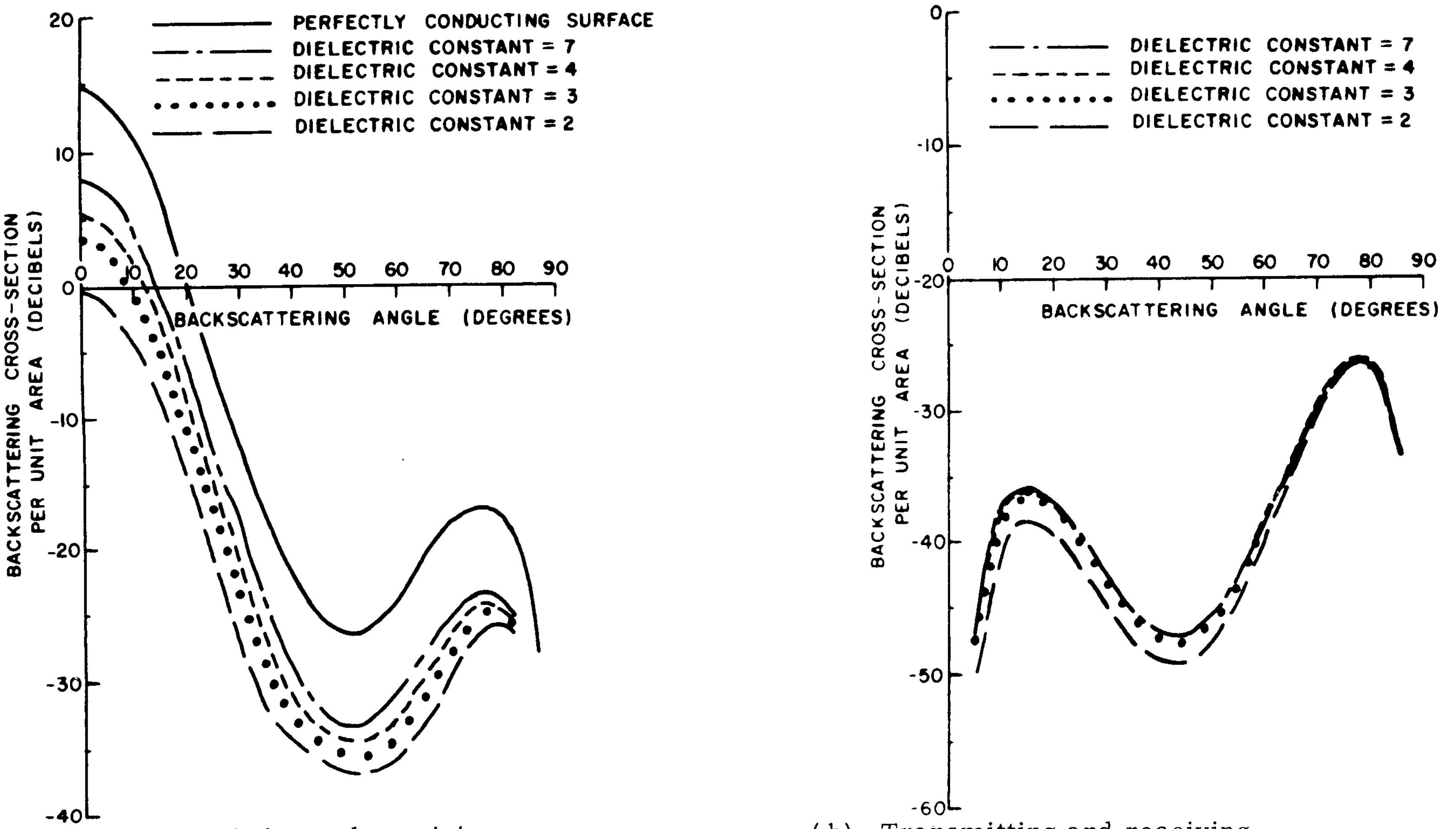

(a) Transmitting and receiving polarizations parallel.

(b) Transmitting and receiving polarizations perpendicular.

Fig. G-3--Predicted backscattering cross section for a pulse-illuminated planetary range ring using linear polarization. RMS surface slope = 10°. Gaussian JPDF for surface height.

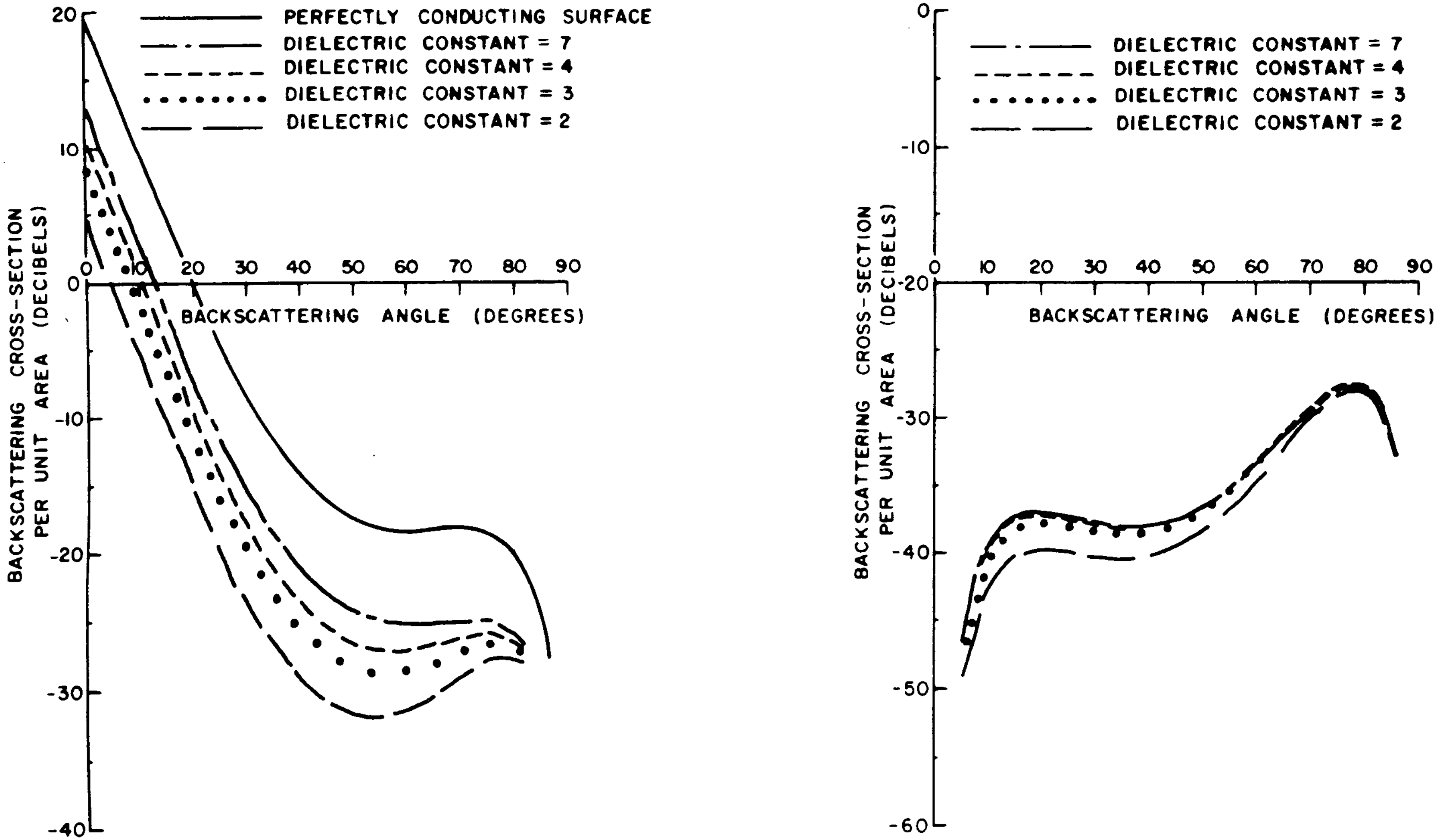

(a) Transmitting and receiving polarizations parallel.

(b) Transmitting and receiving polarizations perpendicular.

Fig. G-4--Predicted backscattering cross section for a pulse-illuminated planetary range ring using linear polarization. RMS surface slope = 10°. Bessel JPDF for surface height.

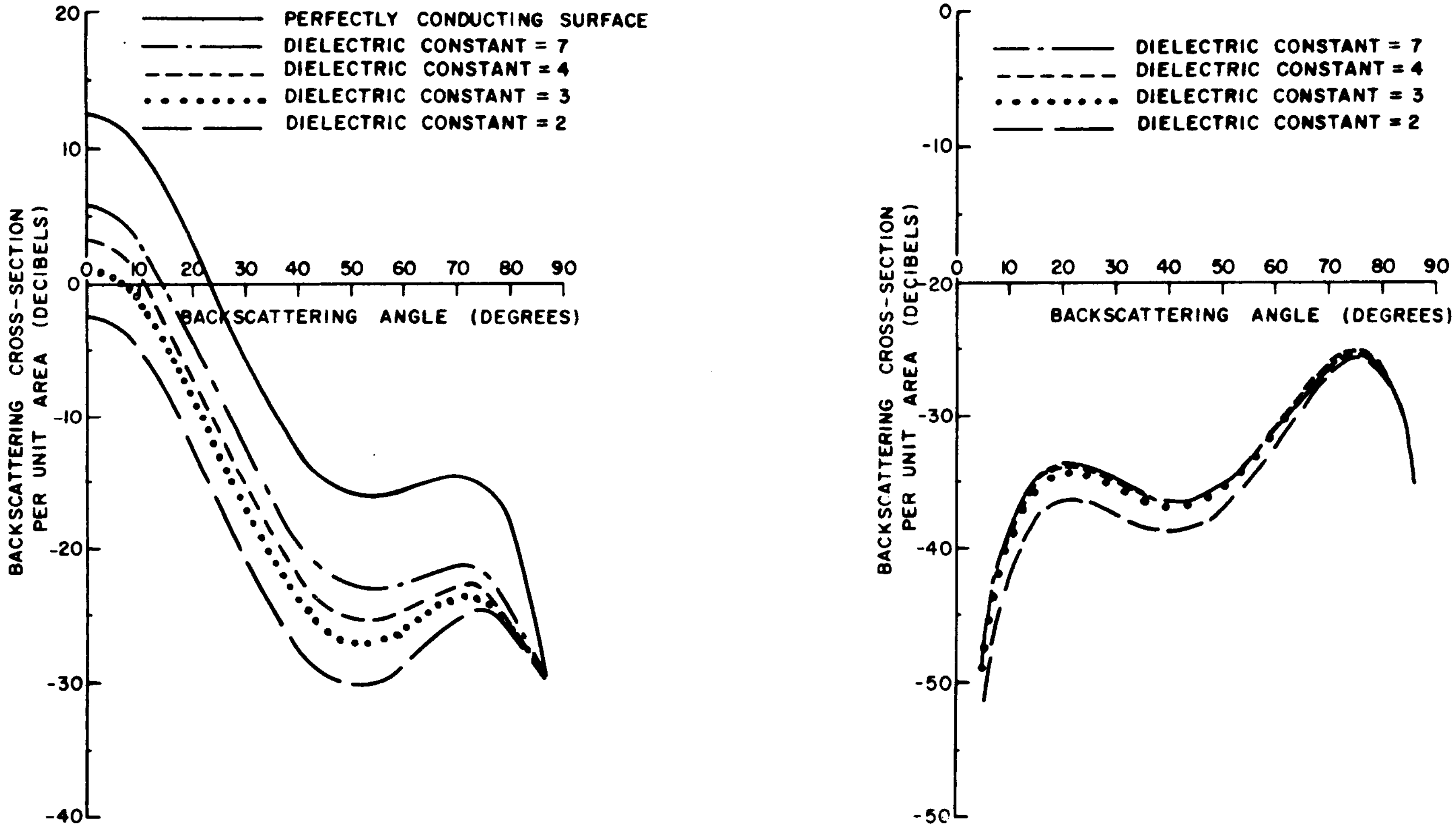

(a) Transmitting and receiving polarizations parallel.

(b) Transmitting and receiving polarizations perpendicular.

Fig. G-5--Predicted backscattering cross section for a pulse-illuminated planetary range ring using linear polarization. RMS surface slope = 12.5°. Gaussian JPDF for surface height.

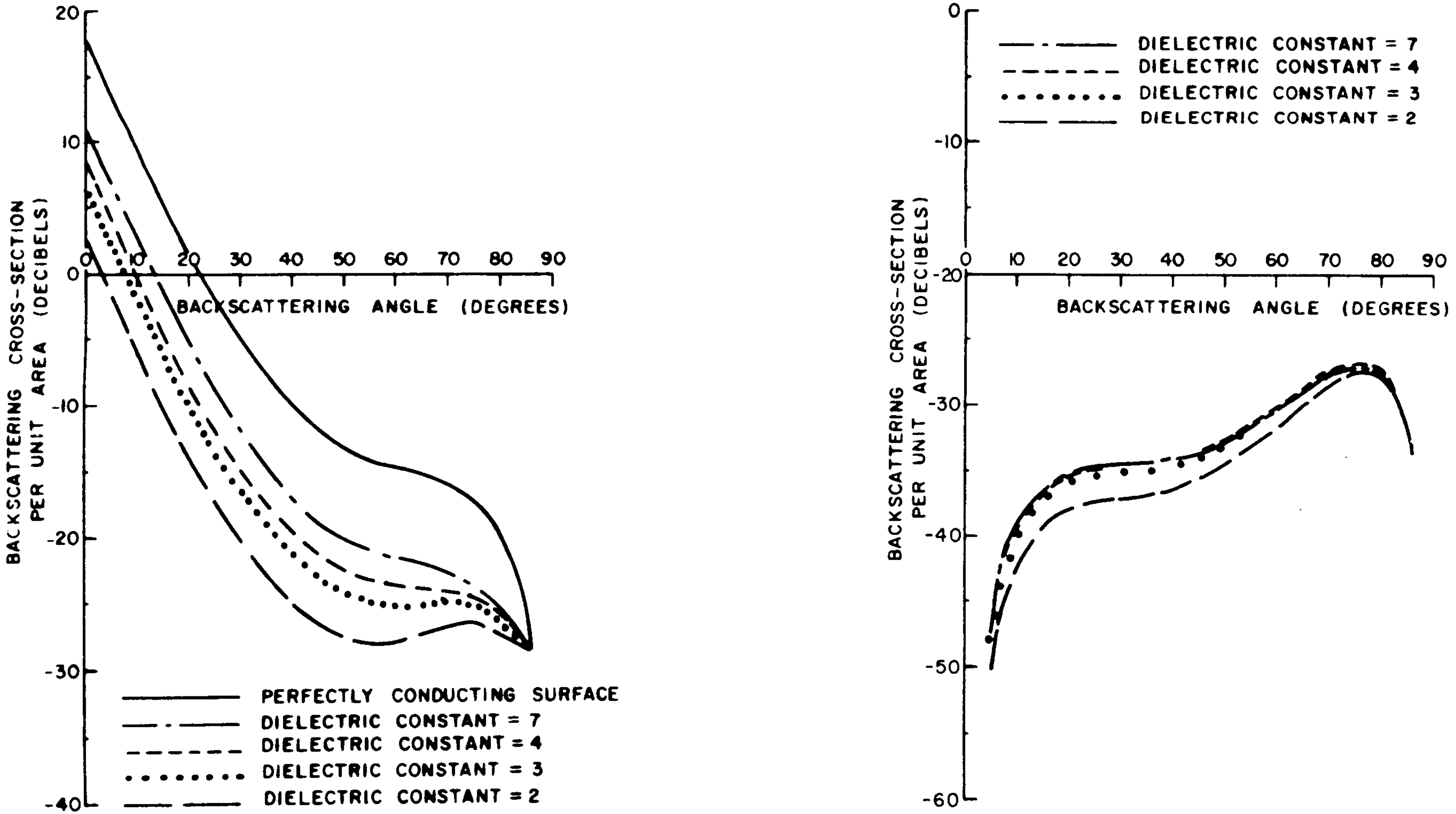

(a) Transmitting and receiving polarizations parallel.

(b) Transmitting and receiving polarizations perpendicular.

Fig. G-6--Predicted backscattering cross section for a pulse-illuminated planetary range ring using linear polarization. RMS surface slope = 12.5°. Bessel JPDF for surface height.

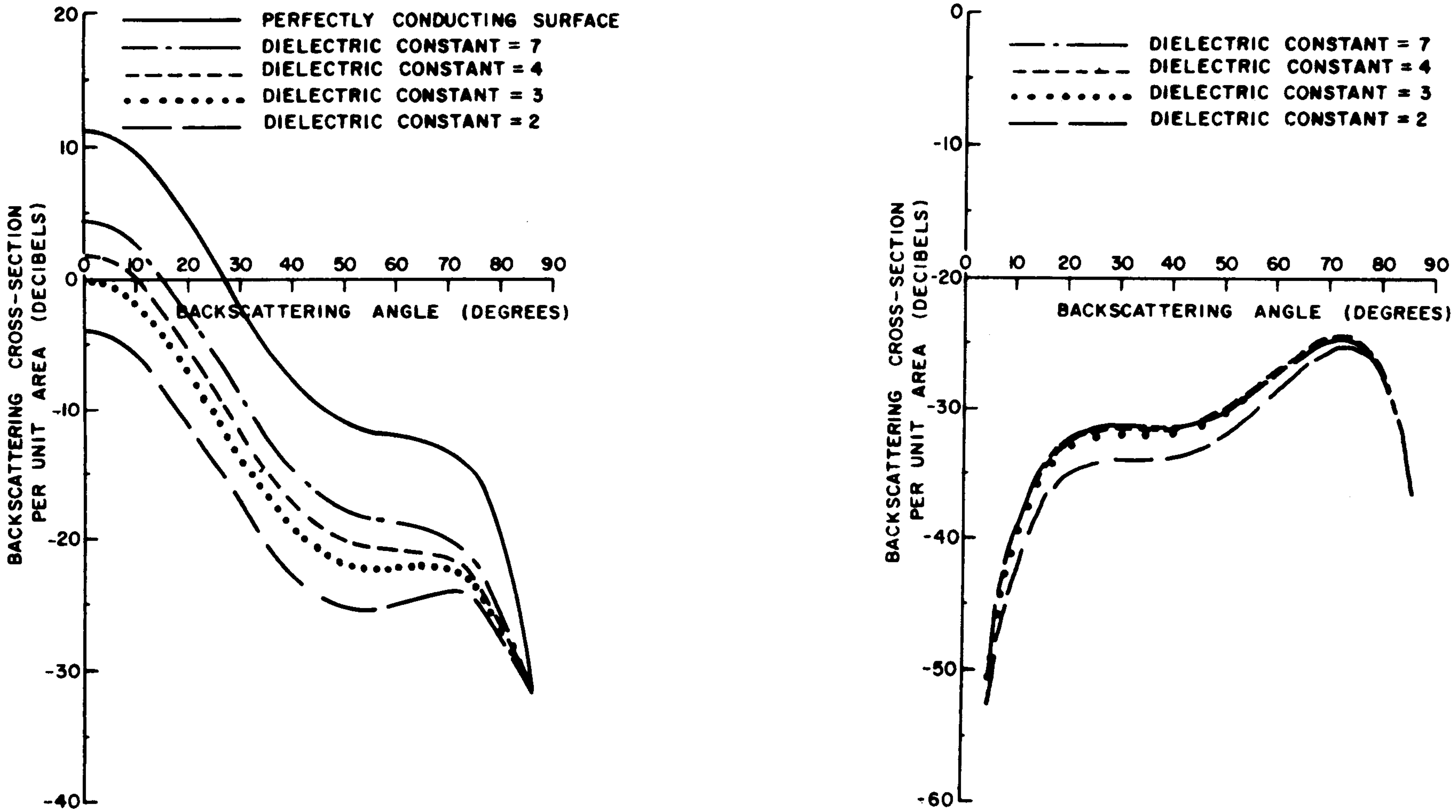

(a) Transmitting and receiving polarizations parallel.

(b) Transmitting and receiving polarizations perpendicular.

Fig. G-7--Predicted backscattering cross section for a pulse-illuminated planetary range ring using linear polarization. RMS surface slope = 15°. Gaussian JPDF for surface height.

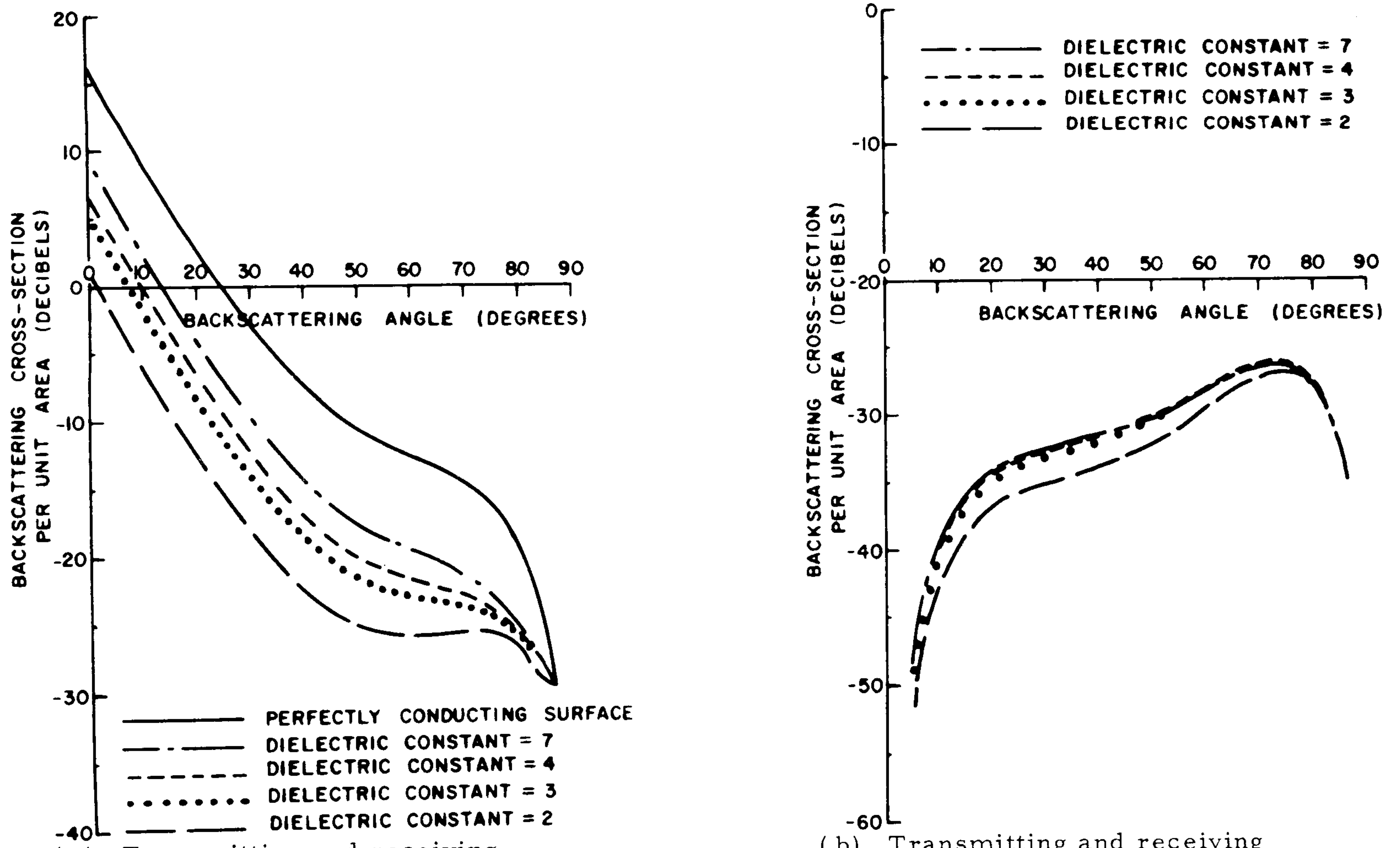

(a) Transmitting and receiving polarizations parallel.

(b) Transmitting and receiving polarizations perpendicular.

Fig. G-8--Predicted backscattering cross section for a pulse-illuminated planetary range ring using linear polarization. RMS surface slope = 15°. Bessel JPDF for surface height.

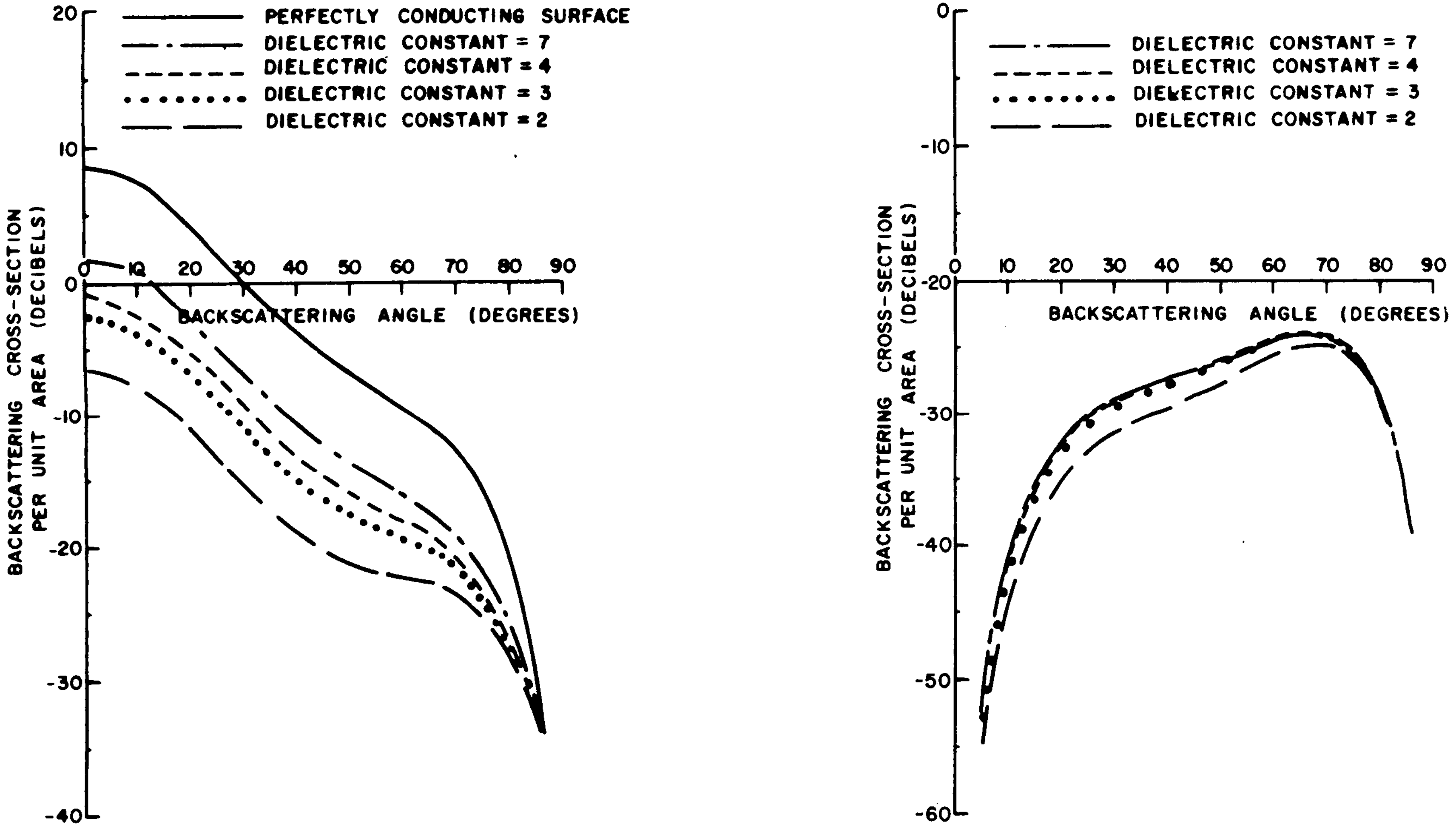

(a) Transmitting and receiving polarizations parallel.

(b) Transmitting and receiving polarizations perpendicular.

Fig. G-9--Predicted backscattering cross section for a pulse-illuminated planetary range ring using linear polarization. RMS surface slope = 20°. Gaussian JPDF for surface height.

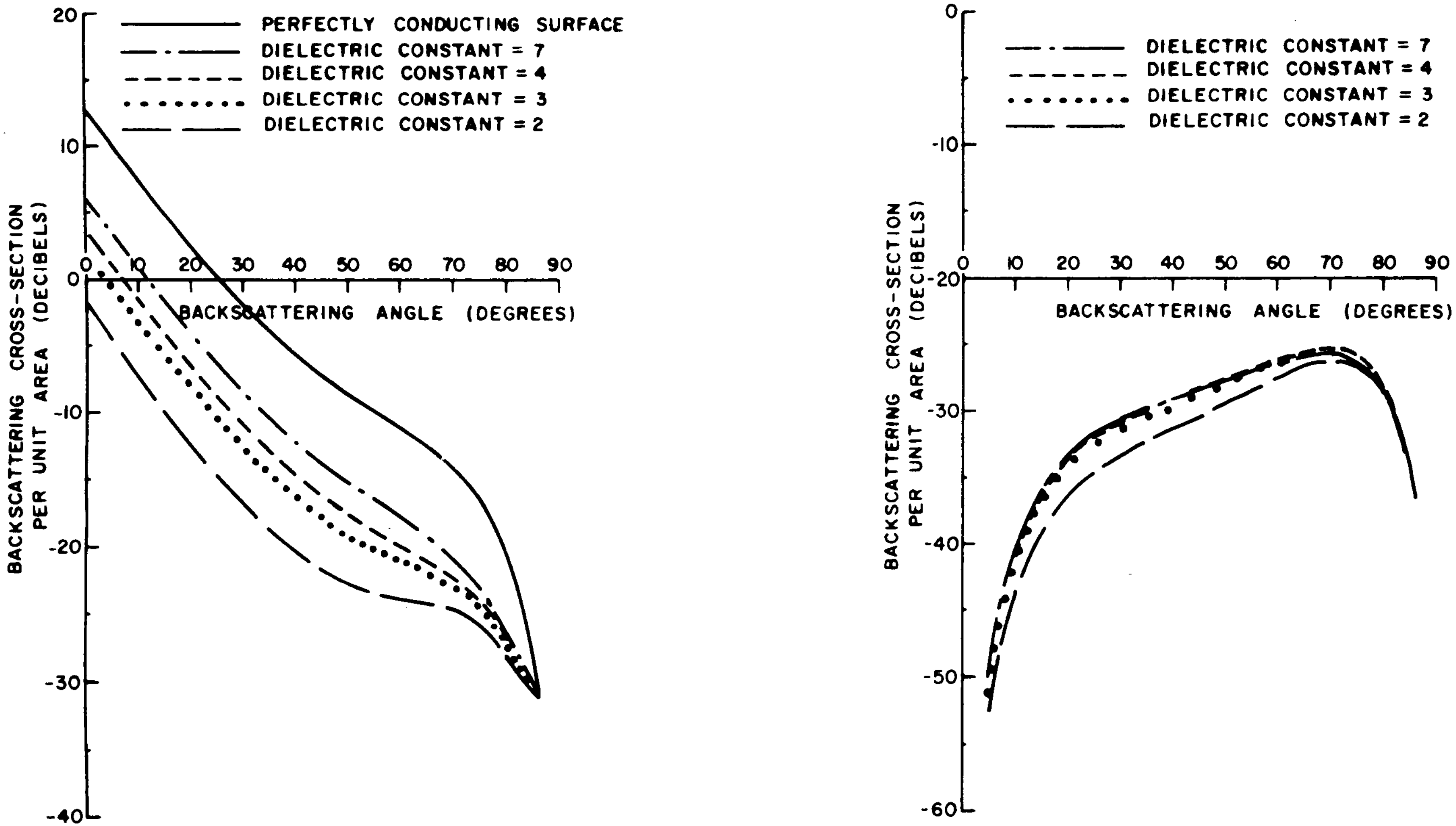

(a) Transmitting and receiving polarizations parallel.

(b) Transmitting and receiving polarizations perpendicular.

Fig. G-10--Predicted backscattering cross section for a pulse-illuminated planetary range ring using linear polarization. RMS surface slope = 20°. Bessel JPDF for surface height.